ARTICLE

Åsa Edfelt · Robin N. Armstrong · Martin Smith
Olof Martinsson

Alteration paragenesis and mineral chemistry of the Tjårrojåkka apatite–iron and Cu (-Au) occurrences, Kiruna area, northern Sweden

Abstract The northern Norrbotten area in northern Sweden, is an important mining district and hosts several deposits of Fe-oxide Cu-Au-type. One of the best examples of spatially, and possibly genetically, related apatite–iron and copper–gold deposits in the region is at Tjårrojåkka, 50 km WSW of Kiruna. The deposits are hosted by strongly sheared and metamorphosed intermediate volcanic rocks and dolerites and show a structural control. The Tjårrojåkka iron deposit is a typical apatite–iron ore of Kiruna-type and the Tjårrojåkka copper occurrence shows the same characteristics as most other epigenetic deposits in Norrbotten. The host rock has been affected by strong albite and K-feldspar alteration related to mineralisation, resulting in an enrichment of Na, K, and Ba. Fe and V were depleted in the altered zones and added in mineralised samples. REE were enriched in the system, with the greatest addition related to mineralisation. Y was also mobile associated with albite alteration and copper mineralisation. The Tjårrojåkka iron and copper deposits show comparable hydrothermal alteration minerals and paragenesis, which might be a product of common host rock and similarities in ore fluid composition, or overprinting by successive alteration stages. Mineralogy and mineral chemistry of the alteration minerals (apatite, scapolite, feldspars, amphiboles, and biotite) indicate a higher salinity and Ba/K ratio in the fluid related to the alterations in the apatite–iron occurrence than in the copper deposit, where the minerals are enriched in F and S. The presence of hematite, barite, and in SO_4 in scapolite suggests more oxidising-rich conditions during the emplacement of the Tjårrojåkka-Cu deposit. From existing data it might be suggested that one evolving system created the two occurrences, with the copper mineralisation representing a slightly later product.

Keywords Sweden · Proterozoic · IOCG · Hydrothermal alteration · Mineral chemistry

Å. Edfelt (✉) · O. Martinsson
Division of Ore Geology and Applied Geophysics,
Luleå University of Technology, 971 87 Luleå, Sweden
E-mail: Asa.Edfelt@ltu.se

R. N. Armstrong
Department of Mineralogy, The Natural History Museum,
Cromwell Road, London, SW3 5BD, UK

M. Smith
Cockcroft Building, University of Brighton, Lewes Road,
Brighton, BN2 4GJ, UK

Introduction

The northern Norrbotten area, northern Sweden (Fig. 1), hosts several economic and subeconomic Fe-oxide and Cu (-Au) deposits and has been described as an Fe-oxide Cu–Au (IOCG) district (Hitzman et al. 1992). The most economically significant deposits of the region are the Kiruna and Malmberget apatite–iron and the Aitik Cu-Au ores. The Tjårrojåkka area is located about 50 km WSW of Kiruna and hosts one of the best examples in Norrbotten of spatially related apatite–iron and copper deposits (Fig. 1). Following an extensive exploration program in 1967–1975, a large number of drill cores are available from the area, but no scientific results on the Tjårrojåkka occurrences have been published to date. The geology of the deposits is briefly described in Ros and Rönnbäck (1971), Grip and Frietsch (1973), Quezada and Ros (1975), Ekström (1978) and Ros (1979). More recently short descriptions of the Tjårrojåkka area have been published in Bergman et al. (2001), Edfelt and Martinsson (2003), Edfelt and Martinsson (2004), and Edfelt et al. (2004).

The geological settings, hydrothermal alteration systematics and mineralising fluid compositions among deposits classified as IOCG-type show a great variation (e.g. Porter 2001; Sillitoe 2003; Hitzman et al. 1992). Detailed descriptions of specific parageneses and mineral associations are important in order to understand the

Fig. 1 Geological map of northern Norrbotten showing the location of major Fe and Cu (-Au) deposits, and the Tjårrojåkka study area (after Bergman et al. 2001). *Inset map*: map of the Fennoscandian Shield with the location of the northern Norrbotten area. *KNDZ* Kiruna-Naimakka deformation zone; *KADZ* Karesuando-Arjeplog deformation zone; *NDZ* Nautanen deformation zone; *PSH* Pajala shear zone
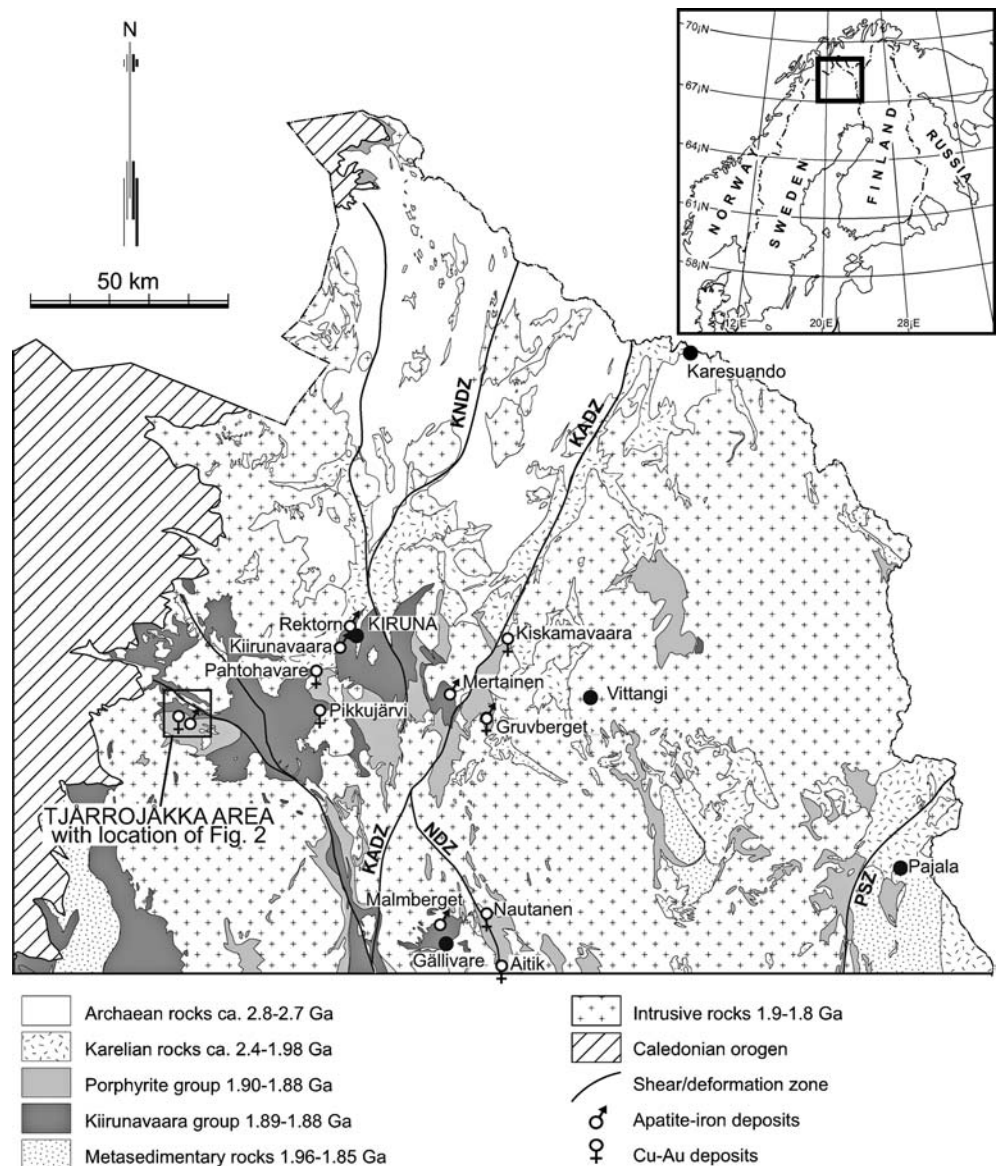
possible genetic relationships between different deposit types within this broad classification. This paper will describe the alteration characteristics of the Tjårrojåkka apatite–iron and Cu (-Au) occurrences in terms of whole-rock geochemistry, mineral chemistry and paragenesis. The mineral chemical data are also used as an indicator of the nature of the hydrothermal fluids involved in the formation of the deposits. These data will be used to examine the relationship between the two occurrences and compare them to other deposits in the region and elsewhere in the world.

Regional geological setting and metallogeny

The Precambrian bedrock in the northern Norrbotten region includes a ca. 2.8 Ga Archaean granitoid-gneiss basement, which is unconformably overlain by a meta-

volcanic sequence of Palaeoproterozoic age (Fig. 1). Stratigraphically lowest in the metavolcanic sequence are rift related 2.5–2.0 Ga Karelian units that are followed by ca. 1.9 Ga Svecofennian successions including several units of metavolcanic and epiclastic rocks. In the central Kiruna area the Svecofennian successions comprise, from the oldest to youngest, the Porphyrite Group, the Kurravaara Conglomerate, the Kiirunavaara Group and the Hauki Quartzite (Allen et al. 2004). Equivalent Palaeoproterozoic units are also found outside the Kiruna area. The calc-alkaline andesite-dominated Porphyrite Group is suggested to be subduction related, while the Kiirunavaara Group has a bimodal character and a geochemical signature resembling within-plate volcanic rocks (Martinsson and Perdahl 1994).

The approximately 10-km thick pile of Palaeoproterozoic volcanic and sedimentary rocks was deformed

and metamorphosed contemporaneously with intrusion of the Haparanda (1.89–1.87 Ga) and Perthite monzonite (1.88–1.86 Ga) granitoid suites (Bergman et al. 2001). These plutonic rocks have a calc-alkaline to alkali-calcic character and are comagmatic with the Svecofennian volcanic rocks (Witschard 1984; Bergman et al. 2001). The Lina Suite comprises ca. 1.79 Ga granites and pegmatites (Skiöld et al. 1988), which are temporally related to Trans-Scandinavian Igneous Belt (TIB) 1 intrusions in the Kiruna-Narvik area (Romer et al. 1994; Romer et al. 1992). A second phase of metamorphism and deformation occurred at least locally at this time (Bergman et al. 2001).

Northern Norrbotten is an important mining province dominated by Fe- and Cu-deposits, with Au as a minor constituent in some of the Cu-occurrences. The main occurrences and their characteristics are summarised in Table 1. The economically most important deposits are the iron ores with an annual production of ca. 31 Mt of ore from the Kiirunavaara and Malmberget deposits (Fig. 1), and a total production of about 1,600 Mt from 10 mines during the last 100 years. Besides magnetite and hematite, most of the iron ores contain significant amounts of apatite. This class of deposits has been named "apatite–iron ores" or "Kiruna type" with the Kiirunavaara deposit being the largest and best-known example. Kiirunavaara contains more than 2,000 Mt of high-grade ore and was first described in detail by Geijer (1910). About 40 apatite–iron ores are known from northern Norrbotten. Individual deposits have an average content of Fe and P varying between 30–65 and 0.05–5%, respectively. Their spatial distribution coincides with that of the Kiirunavaara Group and they are almost exclusively hosted by metavolcanic rocks belonging either to the Kiirunavaara Group or the underlying Porphyrite Group (Martinsson 2003). Ore-elated alteration minerals include albite, scapolite, amphibole, K-feldspar, quartz, and sericite.

Copper was produced intermittently during the seventeenth and eighteenth centuries and recently on a larger scale in the Kiruna area. Sweden's largest sulphide mine, Aitik, is situated in the Gällivare area (Fig. 1). With an annual production of 18 Mt of ore, it is one of the major Cu and Au producers in Western Europe. Although only a few economic sulphide deposits have been found in the northern Norrbotten ore province, a large number of epigenetic Cu–Au occurrences exist in the area. They exhibit large variation in mineralisation style, host rock composition and ore-related hydrothermal alteration.

Most copper deposits are hosted by tuffitic units of the Karelian greenstones and mafic to intermediate volcanic rocks within the Svecofennian porphyries (i.e. the Porphyrite Group and the Kiirunavaara Group).

Table 1 Summary of characteristics of Fe-oxide and Cu–Au deposits in northern Norrbotten

Deposit	Grade and size	Ore minerals and gangue minerals	Host rocks–wall rocks	Alteration minerals	References
Kiirunavaara	>2,000 Mt at >60% Fe, ca. 1% P	Mag, (Hem), Ap, Am	Trachyandesite, rhyodacite	Am, Ab, Bt	Bergman et al. (2001)
Rektorn	20 Mt at 33% Fe, 3.5% P	Hem, Mag, Ap, Qtz, Carb	Rhyodacite, rhyolite	Kfs, Qtz, Ser, Chl, Bt, Tur	Bergman et al. (2001)
Malmberget	660 Mt at 51- 61% Fe, <0.8% P	Mag, Hem, Ap	Trachyandesite, rhyodacite[a]	Ab, Kfs, Bt, Am, Scp	Bergman et al. (2001)
Mertainen	166 Mt at 35% Fe	Mag, Am	Trachyandesite	Ab, Scp, Am	Lundberg and Smellie (1979) Bergman et al. (2001)
Aitik	606 Mt at 0.38% Cu, 0.21g/ton Au	Ccp, Py, Po, (Bn, Mag, Mo), Brt, Bt, Qtz, Grt	Andesitic volcaniclastic[a], Qtz-monzodiorite	Bt, Ser, Kfs, Ep, Grt	Wanhainen et al. (2003)
Pahtohavare	1.68 Mt at 1.89% Cu, 0.88 ppm Au	Ccp, Py, Po, Ab, Carb, Scp	Basaltic tuffite, graphite schist, mafic sill	Ab, Scp, Bt, Carb	Lindblom et al. (1996) Bergman et al. (2001)
Gruvberget	0.2 Mt at 0.5–1% Cu (production)	Ccp, Bn, Mag, (Mo), Kfs, Ep, Carb	Andesite[a]	Ab, Kfs, Scp, Ep, Am, Grt, Px	Frietsch (1966) Lindskog (2001)
Nautanen	0.07 Mt at 1–1.5% Cu (production)	Ccp, Bn, Mag, (Mo), Kfs, Ser, Tur, Grt, Qtz, Am	Andesitic volcaniclastic[a]	Kfs, Bt, Scp, Grt, Ser, Tur, Qtz	Bergman et al. (2001)
Pikkujärvi	5 Mt at 0.61% Cu	Ccp, Bn, Mag, (Mo), Kfs, Tur, Scp	Basalt, Qtz-monzonite	Kfs, Bt, Scp, Tur	Bergman et al. (2001)
Kiskamavaara	3.4 Mt at 0.37% Cu, 0.09% Co	Py, Ccp, Mag, Hem, (Mo), Kfs	Andesite	Kfs, Ser, Scp, Bt, (Tur)	Bergman et al. (2001)

Ab Albite; *Am* amphibole; *Ap* apatite; *Brt* barite; *Bt* biotite; *Carb* carbonate; *Chl* chlorite; *Ep* epidote; *Grt* garnet; *Kfs* K-feldspar; *Px* pyroxene; *Qtz* quartz; *Scp* scapolite; *Ser* sericite; *Tur* tourmaline; *Bn* bornite; *Ccp* chalcopyrite; *Hem* hematite; *Mag* magnetite; *Mo* molybdenite; *Po* pyrrhotite; *Py* pyrite

[a]Suggested precursor of strongly altered/metamorphosed rock Mineral in brackets less common

Some of them display a close genetic and/or spatial relationship to intrusive rocks varying in composition from monzodiorite to granite represented by plutons belonging to the Haparanda and Perthite monzonite suites. Magnetite is a common minor component in many of the deposits and in two cases (Gruvberget and Tjårrojåkka) the copper deposits occur adjacent to major magnetite deposits (Allen et al. 2004; Bergman et al. 2001). Besides structural traps, chemical traps may also be important, with redox reactions involving graphitic schists triggering sulphide precipitation. In addition to Cu, several occurrences also contain Co and/or Au in economic to subeconomic amounts (Martinsson 2000; Bergman et al. 2001).

Ore-related alteration is dominated by K-feldspar, albite, biotite, and scapolite with amphibole, carbonate, tourmaline, garnet, and sericite as locally important minerals. In most deposits the paragenetic sequence from oldest to youngest is: scapolite + biotite → albite → carbonate, or: scapolite + biotite → K-feldspar → sericite ± tourmaline. Stilbite and chabazite may be late phases occurring in druses and veins together with calcite. Ore minerals formed mainly at the intermediate or late stages of alteration. Geochrono-

logical data from Cu–Au deposits and hydrothermal alteration in the northern Norrbotten ore province demonstrates two major events of ore formation at ca. 1.87 and 1.77 Ga, respectively (Billström and Martinsson 2000; Edfelt 2003). The importance of saline hydrothermal fluids in the genesis of regional albite–scapolite alteration and the nature of the ore deposits in the northern Norrbotten ore province and adjacent Karelian areas in northern Finland and Norway has been emphasised by Frietsch et al. (1997). Highly saline fluid inclusions with 30–45 eq.wt% NaCl and depositional temperatures of 500–300°C are recorded for the Cu–Au deposits in this region (Ettner et al. 1993; Lindblom et al. 1996; Broman and Martinsson 2000). High Ca contents characterise ore fluids from most Cu–Au occurrences, which might be an expression of added components from evaporitic sediments within the Karelian greenstones that contributed to the salinity of the mineralising fluids (Wanhainen et al. 2003).

Geology of the Tjårrojåkka area

The geology in the Tjårrojåkka area is dominated by metamorphosed mafic to intermediate extrusive and intrusive rocks (Fig. 2). The stratigraphically lowest unit comprises metaandesites and metadolerites that are overlain by metabasalts. The metabasalts and metadolerites in the area have the same chemical signature

Fig. 2 Generalised geology of the Tjårrojåkka area with location of the Tjårrojåkka iron and copper deposits and minor occurrences. *Inset map*: drill holes at the Tjårrojåkka deposits with the investigated profiles indicated. Sections 400W and 320E shown in Figs. 3 and 4, respectively
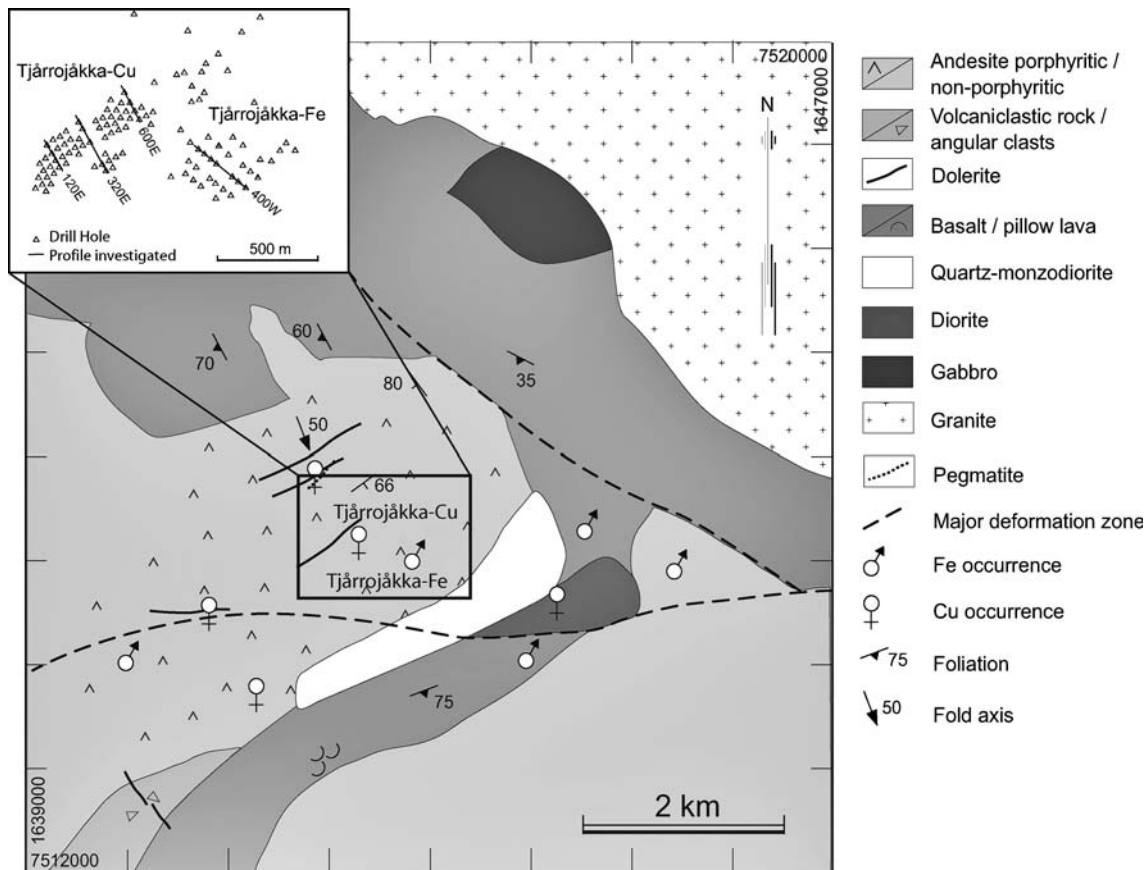
and have been interpreted to have formed from the same magma with the dolerites acting as feeder dykes for the overlying basaltic unit (Edfelt 2003). Intrusions of gabbroic to quartz-monzodioritic composition crosscut the andesites and basalts. The rocks are metamorphosed in epidote-amphibolite facies, based on mineral assemblages (hornblende + plagioclase ± epidote ± quartz) (Spear 1993) of non-mineralised basic rocks (metabasalt and -dolerite). They have been strongly affected by albite, scapolite, and K-feldspar alteration that is more intense in the vicinity of deformation zones and mineralisation. From textural relationships (scapolite porphyroblasts growing over the metamorphic foliation in metabasalts and -dolerites) the regional alterations are interpreted as being temporally later than the metamorphism. Based on geochemistry the metaandesites resemble the intermediate rocks of the Svecofennian Porphyrite Group, while the metadolerites and -basalts have a more primitive signature and cannot be correlated with any known volcanic sequence in Norrbotten (Edfelt 2003).

Rocks of the area, which are located within a splay off of a regional NW–SE trending deformation zone (Fig. 1), have undergone at least three stages of deformation including two compressional events (Edfelt 2003). The first compressional episode created NE–SW striking foliation parallel to the strike of the Tjårrojåkka deposits. It was followed by the development of an E–W trending deformation zone identified from aeromagnetic data showing a low magnetic anomaly and parallel foliation (shearing) in outcrops. The third deformation stage is characterised by ENE–WSW compression seen in folding in the central part of the area. The compressional stages can also be correlated with the regional tectonics in Norrbotten (cf. Bergman et al. 2001). Several structurally controlled Fe- and Cu-occurrences occur in the area (Sandrin and Elming 2003) of which the largest are the Tjårrojåkka magnetite–apatite (Tjårrojåkka-Fe) and the Tjårrojåkka copper-gold (Tjårrojåkka-Cu) occurrences located 750 m apart.

The Tjårrojåkka-Fe deposit, comprising massive magnetite with minor disseminated copper, was discovered through airborne magnetic measurements in 1963 by the Geological Survey of Sweden. A drilling program was initiated in 1967 and continued for 3 years during which some copper-bearing boulders and outcrops were found, and the Tjårrojåkka-Cu prospect was discovered. Between 1970 and 1975, 62 drill holes were drilled into the copper deposit. The Tjårrojåkka-Fe deposit is hosted by strongly sheared intermediate metavolcanic rocks and less deformed metadolerites. It consists of a massive magnetite core surrounded by a fractured host rock with apatite–magnetite veins filling the fractures (breccia) known to a depth of 400 m. The calculated tonnage for the apatite–iron deposit is 52.6 Mt at 51.5% Fe (Quezada and Ros 1975) with locally up to 3% Cu in some sections. The Tjårrojåkka-Cu occurrence, which is characterised by copper sulphides with minor quantities of magnetite, is hosted by the same rocks, localised in a

30 m wide and 700 m long zone, striking NE and dipping approximately 85° towards north. The deposit is estimated to contain 3.23 Mt at 0.87% Cu (cut-off 0.4%) (Ros 1979).

Sampling and analytical methods

Four drill sections, one in the apatite–iron ore and three in the copper deposit (Fig. 2), were logged and sampled. Seventy-six thin sections representing different rock and alteration types were initially examined in transmitted and reflected light at Luleå University of Technology and subsequently at the Natural History Museum, London using a Jeol 5900LV scanning electron microscope (SEM). SEM observations were made using a back-scattered electron detector (BSE), with an accelerating voltage of 20 kV and a beam current of 1 nA measured specimen current in pure cobalt metal.

Mineral analyses were performed using a Cameca SX50 WDS electron microprobe at the Natural History Museum, London, with the technique described in Potts et al. (1995). The analytical conditions and standards used for different minerals are available in Edfelt (2003) and the samples analysed are described in Appendix. Silicate analyses were carried out using an accelerating voltage of 15 or 20 kV, a beam current of 20 nA, and a 5-μm beam diameter. Apatites were analysed using an accelerating voltage of 15 kV, a beam current of 20 nA, and a 5-μm beam diameter. For sulphides and oxides a 1-μm beam diameter, an accelerating voltage of 15 or 20 kV, and a beam current of 20 nA were used, except for one set of sulphide analyses for which a 60 nA beam current was used. Different pure metals, natural minerals and synthetic glasses were used as standards. Interferences between X-ray peaks for Ba/Ti, Ce/Ti, Ce/Ba, Nd/Ce, Co/Fe, F/Ce, Mo/S and V/Ti were corrected empirically using previously collected data from standards.

Whole-rock analyses for major and trace elements were carried out on 89 drill core samples at Activation Laboratories Ltd in Canada. The major elements were analysed using the inductively coupled plasma method (ICCP-OES), while trace elements were analysed by inductively coupled plasma mass spectrometry (ICCP-MS) and instrumental neutron activation analysis (INAA).

Mineralisation and hydrothermal alteration

The main ore and alteration minerals and styles are summarised in Table 2. Cross sections through the Tjårrojåkka-Fe (400W) and Tjårrojåkka-Cu deposits (320E) (cf. Fig. 2), showing the relationships between mineralisation and main alteration types, are presented in Figs. 3 and 4, respectively. The apatite–iron ore (Tjårrojåkka-Fe) consists of a massive core (60–67% Fe and 0.5–1.3% P) surrounded by a breccia (25–60%

Table 2 Main ore and alteration minerals and styles in the Tjärrojåkka-Fe and Tjärrojåkka-Cu occurrences

Mineral	Associated minerals	Style	Location	Spatial relation to Cu-mineralis-ation	Relative time relationship to main magnetite and copper ore-forming stages
Magnetite	Ab, Scp, Pl, Bt, Ap, Py, Ccp	Massive, veins and disseminated	In breccia surrounding the massive magnetite ore at Tjärrojåkka-Fe; footwall of Tjärrojåkka-Cu; disseminated with Ab alteration	Close to none	Massive Mag ore pre Cu-mineralisation, veins mostly pre Cu-mineralisation, in places syn Cu-mineralisation (intergrown with Ccp)
Hematite	Mag	Veins and disseminated	In and around the massive magnetite ore of Tjärrojåkka-Fe; footwall of Tjärrojåkka-Cu	Some	Post massive Mag, pre (-syn) Cu-mineralisation
Chalcopyrite	Bn, Py, Mag, Ap, Kfs, Am, Qtz	Veins and disseminated	In the massive magnetite ore and in the surrounding breccia at Tjärrojåkka-Fe; mineralised part of Tjärrojåkka-Cu	Close	Post massive Mag, syn Cu-mineralisation
Bornite	Ccp	Veins and disseminated	In the massive magnetite ore and in the surrounding breccia at Tjärrojåkka-Fe; mineralised part of Tjärrojåkka-Cu	Close	Post massive Mag, syn Cu-mineralisation
Pyrite	Ccp, Carb, Zeol	Veins and disseminated	In the breccia at Tjärrojåkka-Fe; mineralised part of Tjärrojåkka-Cu	Close	Post massive Mag, syn-post Cu-mineralisation
Albite	Mag	Pervasive	Around the massive magnetite ore of Tjärrojåkka-Fe; footwall of Tjärrojåkka-Cu; between the copper and iron deposits	None	Syn-post massive Mag, pre Cu-mineralisation
Tremolite	Ap, (Carb)	Fracture filling, veinlets	In massive magnetite ore at Tjärrojåkka-Fe	None	Syn-post massive Mag, pre Cu-mineralisation
Mg-hornblende	Kfs, Ccp, Py, Mag	Disseminated, porphyroblasts, and veinlets	Everywhere in wall rock	Close to none	Post massive Mag, syn-post Cu-mineralisation
Tschermakite	Kfs, Ccp, Py, Mag	Disseminated, porphyroblasts, and veinlets	Everywhere in wall rock	Close to none	Post massive Mag, syn-post Cu-mineralisation
Actinolite	Kfs, Ttn	Veins, veinlets	Everywhere in wall rock	Close	Post massive Mag, syn-post Cu-mineralisation
Apatite	Mag, Am, Ccp, Bn, Py, Carb	Veins, disseminated	Inside and around the magnetite ore at Tjärrojåkka-Fe; footwall of Tjärrojåkka-Cu	Some	Syn-post massive Mag, pre- main Cu-mineralisation
Biotite	Scp, Mag, (Kfs), Pl	Pervasive	Related to scapolite and K-feldspar alteration in both deposits	Some	Mainly pre (-syn) Cu-mineralisation
Scapolite	Mag, Bt, Am	Porphyroblasts, veins	In dolerites; locally in wall rock around massive magnetite ore at Tjärrojåkka-Fe; in hanging wall of Tjärrojåkka-Cu	Some	Post massive Mag, pre-main Cu-mineralisation
K-feldspar	Act, Mg-Hbl, Ts, Ep, Ccp, Bn, Mag, Qtz, Ttn	Pervasive and in veins	Locally in the wall rock around at Tjärrojåkka-Fe; in the mineralised zone of Tjärrojåkka-Cu	Close	Post massive Mag, syn Cu-mineralisation
Titanite	Kfs, Am	In veins with Am + Kfs	In K alteration around magnetite ore at Tjärrojåkka-Fe; hanging wall of Tjärrojåkka-Cu	Close	Post massive Mag, syn-post Cu-mineralisation
Quartz	Kfs, Am, Ccp, Bn, Carb	Veins	Everywhere in wall rock	Some	Syn-post main ore stages

Table 2 (Contd.)

Mineral	Associated minerals	Style	Location	Spatial relation to Cu-mineralis-ation	Relative time relationship to main magnetite and copper ore-forming stages
Epidote	Kfs, Am, Qtz, Carb	Patches, porphyroblasts, and veinlets (often fracture-controlled)	Everywhere in wall rock	None	Post main ore stages
Fluorite	Musc	Infilling in vugs, along foliation plane	Footwall of Tjårrojåkka-Cu, in periphery of main mineralised zone	None	Post main ore stages
Carbonates	Am, Qtz, Ccp, Zeol	Veinlets, veins	Both in the breccia and in the massive magnetite ore at Tjårrojåkka-Fe; in the footwall of Tjårrojåkka-Cu (more abundant to E)	None	Post main ore stages
Zeolites	Py, (Ccp), Am, Ep, Kfs, Carb	Fracture-contolled, often in reactivated veins	In the breccia around the massive magnetite ore at Tjårrojåkka-Fe; in mineralised zone n the Tjårrojåkka-Cu (more abundant to E)	None	Post main ore stages

Ab Albite; *Act* actinolite; *Ap* apatite; *Bt* biotite; *Carb* carbonate; *Chl* chlorite; *Ccp* chalcopyrite; *Ep* epidote; *Kfs* K-feldspar; *Mag* magnetite; *Mg-Hbl* magnesium-hornblende; *Musc* muscovite; *Pl* plagioclase; *Py* pyrite; *Qtz* quartz; *Scp* scapolite; *Ttn* titanite; *Tr* tremolite; *Ts* tschermakite; *Zeol* zeolite

Fe and 0.4–3% P) with low-grade copper mineralisation (Bergman et al. 2001), whereas the Tjårrojåkka-Cu consists of an elongated body of disseminated copper mineralisation with magnetite–apatite veining in the footwall. Albite, scapolite, and K-feldspar alteration has strongly affected the host rock to both deposits.

Mineralisation

Tjårrojåkka-Fe

Outcrop and drill core investigations indicate that the Tjårrojåkka-Fe deposit was the first of the occurrences to form since copper sulphides occur in fractures and veins crosscutting the massive magnetite. Magnetite is by far the most common ore mineral in the Tjårrojåkka-Fe deposit with minor hematite occurring as veins cutting the magnetite or as partly hematite-altered magnetite grains. Within the massive magnetite ore, veinlets of red or green apatite, tremolite, and carbonate fill fractures (Fig. 5a). Chalcopyrite, bornite, pyrite and minor molybdenite occur as veins and disseminations in the breccia and more rarely in fractures in the massive magnetite body. Gold (electrum) and silver telluride are trace minerals found in chalcopyrite (Fig. 5b). Based on textural relationships the sulphides in general post-date the massive magnetite, but do in some cases occur intergrown with magnetite in the massive ore and in veins in the breccia.

Tjårrojåkka-Cu

The Tjårrojåkka-Cu deposit essentially consists of chalcopyrite, bornite, pyrite, and magnetite as disseminations, patches and in veinlets, locally with disseminated molybdenite. Magnetite occurs in footwall and is cut by later chalcopyrite (Fig. 5c) and carbonate veinlets. The magnetite in some cases exhibits martite replacement textures (Fig. 5d). Chalcopyrite and bornite occur as single grains or intergrown and are mainly associated with pervasive K-feldspar alteration and veins of amphibole ± K-feldspar ± quartz ± magnetite ± carbonate in both metaandesites and metadolerites. Chalcopyrite has also been identified intergrown with pyrite and magnetite. Bornite occurs in the part of the mineralisation richest in copper, while pyrite is more abundant in the eastern part of the deposit and at deeper levels. Silver telluride, silver sulphide, and native gold occur as micron-sized minor phases. Gold has been observed in quartz in a vein together with amphibole and chalcopyrite. Ekström (1978) also observed gold as inclusions in silicates associated with chalcocite and bornite. Chalcocite and covellite have been observed as secondary minerals replacing chalcopyrite and bornite (Ekström 1978) and locally oxidation of copper sulphides has resulted in the formation of malachite and chrysocolla.

416

Fig. 3 Cross section through Tjårrojåkka apatite–iron ore (profile 400W) showing the relation between the magnetite body, breccia, and alteration types. Alteration zones established based on geochemistry and visible appearance of alteration minerals. *Ccp* chalcopyrite; *Bn* bornite
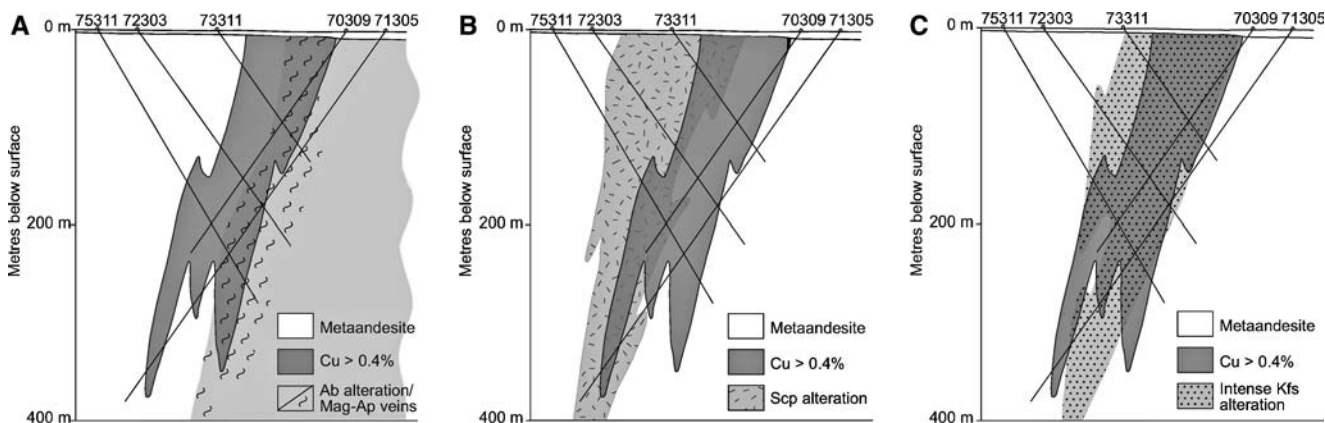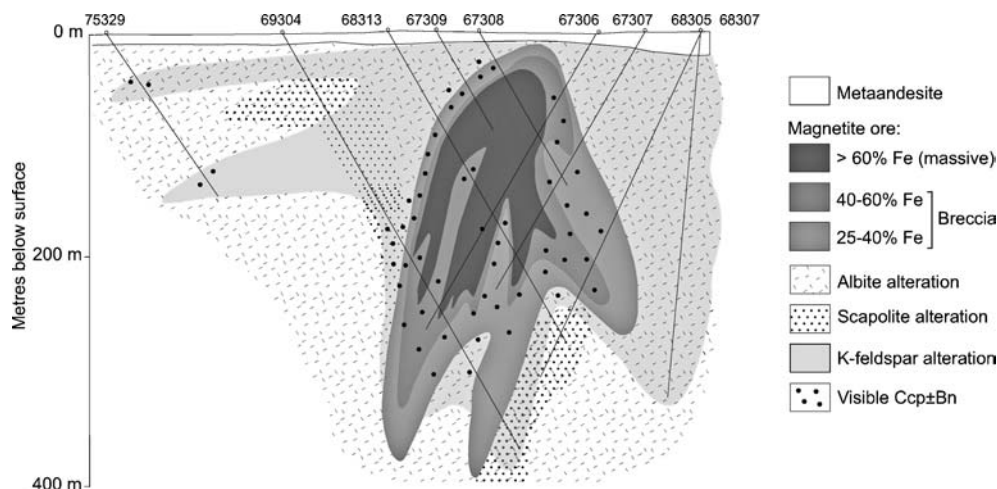

Fig. 4 Cross section through the Tjårrojåkka-Cu deposit (profile 320E) showing the relationships between copper mineralisation and main alteration types. Alteration zones established based on geochemistry and visible appearance of alteration minerals. **a** Albite (*Ab*) altered footwall with overprinting magnetite (Mag)-apatite (Ap) veins. **b** Scapolite (*Scp*) altered hanging wall. **c** Intense K-feldspar (*Kfs*) alteration

Hydrothermal alteration

The hydrothermal alteration assemblages at Tjårrojåkka are highly variable with several of the alteration minerals occurring in numerous generations and settings, overlapping alteration stages, and with reactivation of already pre-existing veins, indicating a complex, long history of fluid activity in the area. The most widespread alteration minerals are albite, magnetite, apatite, scapolite, biotite, K-feldspar, and clinoamphiboles (tremolite, actinolite, Mg-hornblende, and tschermakite). The paragenetic evolution of the Tjårrojåkka deposits is illustrated in Fig. 6a, b. The alteration paragenesis in the two occurrences is similar, with albite forming at an early stage associated with magnetite and apatite. Scapolite was formed mainly before the main Cu-sulphide stage and is generally accompanied by biotite. The albitised and scapolitised rocks are overprinted by later K-feldspar alteration, which is spatially associated with copper-bearing sulphides. Several different types and generations of amphibole occur, both associated with magnetite and copper mineralisation and in post-mineralisation assemblages. Epidote and zeolites were the last phases to form from post main-ore stage low-temperature fluids.

Tjårrojåkka-Fe

The wall rock adjacent to the Tjårrojåkka apatite–iron deposit has been affected by extensive and pervasive albite alteration giving the rock a light grey or reddish colour due to hematite staining. Albite + magnetite alteration is particularly well developed in the area between the apatite–magnetite and the copper deposit. Scapolite occurs locally as porphyroblasts and later veinlets. The albitised and scapolitised rocks are overprinted by locally pervasive K-feldspar alteration and veins of K-feldspar + Mg-hornblende ± titanite ± quartz ± magnetite ± sulphides. Epidote is common together with K-feldspar, as late veinlets (Fig. 5e) and as an alteration of amphibole (Mg-hornblende). Amphibole (principally actinolite) also occurs in late veins cutting epidote. Allanite occasionally occurs in the matrix associated with epidote. Quartz veins have been observed in two generations. Carbonate veins (usually calcite), sometimes with zeolites ± pyrite, generally
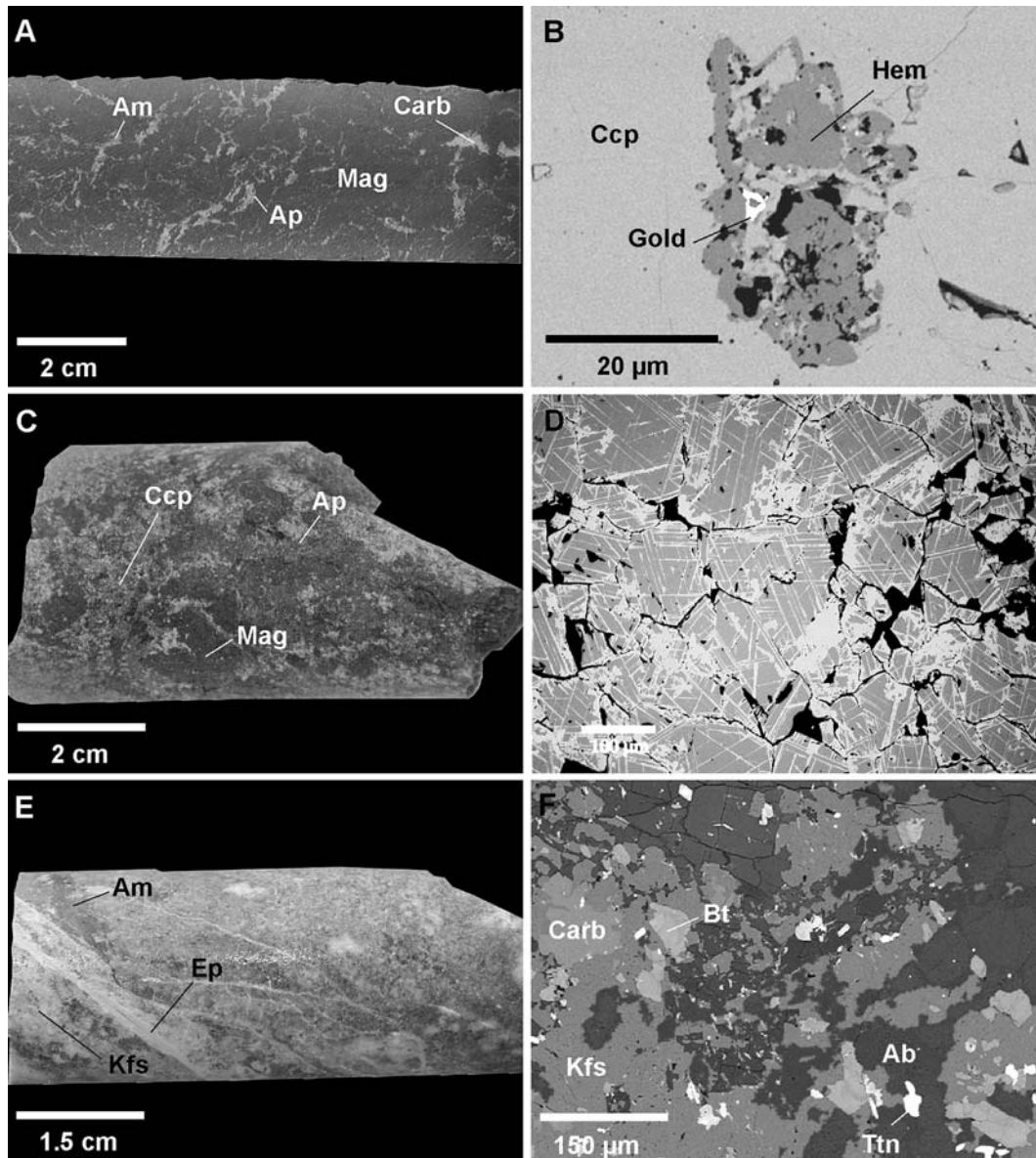
Fig. 5 Photographs of alteration and mineralisation types and textures. **a** Typical massive magnetite ore with apatite, amphibole (tremolite) and carbonate infill from the Tjårrojåkka-Fe deposit. **b** Chalcopyrite with gold and hematite as late infill in fractures in massive magnetite in the Tjårrojåkka-Fe deposit (BSE image). **c** Chalcopyrite crosscutting magnetite in the footwall of the Tjårrojåkka-Cu deposit. **d** Martite (*light grey*) replacing magnetite (*darker grey*) in a vein in the footwall of the Tjårrojåkka-Cu deposit. **e** Epidote veinlets crosscutting K-feldspar-amphibole alteration in porphyritic andesite in the Tjårrojåkka-Cu deposit. **f** Albite altered to K-feldspar in the Tjårrojåkka-Cu deposit (BSE image). *Ab* albite; *Am* amphibole; *Ap* apatite; *Bt* biotite; *Carb* carbonate; *Ep* epidote; *Kfs* K-feldspar; *Ttn* titanite; *Ccp* chalcopyrite; *Hem* hematite; *Mag* magnetite

represent the final stage of infill in existing veins and vugs, or have exploited pre-existing fractures.

Tjårrojåkka-Cu

The footwall to the copper deposit is characterised by pervasive albite alteration overprinted by veins of mag- netite and red, green, white or rare blue apatite (Fig. 4a). K-feldspar post-dates the albite alteration (Fig. 5f). Scapolite (porphyroblasts and veins) was formed at an early stage in the hanging wall (Fig. 4b), subsequently overprinted by pervasive K-feldspar alteration, and has affected the metadolerites to a greater extent than the metaandesites. Amphibole occurs in several generations as porphyroblasts, in monomineralic veins, or together with K-feldspar ± titanite ± quartz ± carbonate ± chalcopyrite ± bornite. The porphyroblasts contain inclusions of quartz, K-feldspar, plagioclase and iron oxide. Biotite occurs together with scapolite and is commonly affected by later chlorite alteration. Epidote occurs as patches in the matrix, together with K-feldspar ± amphibole ± carbonate ± quartz in veins or as a late mineral phase cutting all the earlier phases in thin vein- lets. Zeolites (stilbite and chabazite) are fracture-con- trolled post-ore stage minerals sometimes occurring in earlier formed veins of amphibole ± epidote ± car-

Fig. 6 Simplified paragenetic sequence of main ore and alteration minerals in the Tjårrojåkka apatite–iron (**a**) and Tjårrojåkka copper (**b**) occurrences

A TJÅRROJÅKKA-Fe   Magnetite stage   Copper sulphide stage   Post main ore stage

Magnetite — M   V
Hematite — VL
Chalcopyrite — V+D
Bornite — V+D
Pyrite — V+D   F
Molybdenite — Loc
Gold — Loc
Apatite — VL   V
Scapolite — P+V
Albite — P
Plagioclase — P?
K-feldspar — P+V
Tremolite — VL
Mg-hornblende/Tschermakite — P+V
Biotite — P+V
Titanite — V
Quartz — V
Epidote — F+VL
Carbonate — VL   VL
Zeolites — F

B TJÅRROJÅKKA-Cu   Magnetite stage   Copper sulphide stage   Post main ore stage

Magnetite — M   V
Hematite — VL
Chalcopyrite — V+D
Bornite — V+D
Pyrite — V+D   F
Molybdenite — Loc
Gold — Loc
Apatite — V
Scapolite — ?   P+V
Albite — P
K-feldspar — P+V
Mg-hornblende/Tschermakite — P+V
Actinolite — V
Biotite — P
Titanite — V
Quartz — V
Epidote — F+VL
Carbonate — VL
Zeolites — F

M massive; *V* in veins; *VL* veinlets; *P* pervasive; *F* fracture filling; *D* disseminated; *Loc* locally occurring; *?* uncertain
Solid line = major mineral forming event
Hatched line = minor mineral forming event
The length of the line is not in exact proportion with the time interval of the alteration.

bonate ± chalcopyrite ± pyrite. Fluorite has been observed in profile 600E in association with sericite and pyrite. REE minerals comprise allanite, occurring as rims on epidote, and late REE-carbonates in the magnetite–apatite altered footwall. Barite (associated with Cu-sulphides and in K-feldspar), thorite (intergrown with chalcopyrite or epidote), and zircon (in apatite and veins of chalcopyrite + feldspar + quartz) are minor hydrothermal constituents also observed in the copper deposit.

Whole-rock geochemistry

Geochemical analyses were performed on drill core samples to characterise the mass transfer during mineralisation and different types of alteration. Although attempts were made to sample least altered rocks, all samples exhibit some effect of alteration and/or meta-

morphism; hence the geochemical data do not record pristine magmatic features of the rock which in turn makes the mobile element interpretation difficult.

Major and minor elements

The host rocks to the Tjårrojåkka deposits show large variation in many of the major and minor elements due to the intense hydrothermal alteration (Table 3). The SiO_2 content of the intermediate rocks varies between 50.16 and 67.86 wt% with total alkalis ($Na_2O + K_2O$) from 6.11 to 11.26 wt%. The Fe_2O_3(tot) contents range between 3.19 and 17.84 with TiO_2 reaching a maximum of 0.92 wt%. The Zr content shows large variation from 67 to 439 ppm. The widespread potassic alteration is characterised by elevated values of K_2O (max. 8.96 wt%) and BaO (max. 0.5 wt%), and the sodic

Table 3 Major and trace element whole-rock geochemical data for representative rocks

Rock type	andesite	andesite	andesite	andesite	andesite	andesite	dolerite	dolerite
Alteration	Least altered	Ab altered	Ab altered	Kfs altered	Kfs altered	mineralised	unmineralised	mineralised
Drill hole	Reference sample	68301	70309	68313	74319	74319	69306	74320
m along hole		123.8–124.05	21.35–21.57	76.60–76.85	79.74–80.02	200–208	155.0–162.0	153–156
wt%								
SiO_2	57.09	57.63	61.58	53.72	58.80	59.82	47.68	46.71
TiO_2	0.697	0.699	0.596	0.705	0.658	0.915	1.882	1.759
Al_2O_3	17.56	16.73	16.20	16.06	16.16	15.93	15.08	15.40
Fe_2O_3 (tot.)	9.32	9.42	4.46	10.60	6.93	5.29	14.67	14.01
MnO	0.107	0.046	0.073	0.099	0.097	0.100	0.053	0.328
MgO	2.2	3.25	2.05	3.21	2.37	1.64	7.33	6.21
CaO	4.13	1.7	3.64	4.01	3.95	2.56	2.59	7.53
Na_2O	3.41	6.97	7.15	3.65	3.63	2.11	4.84	2.92
K_2O	4.07	2.46	1.13	5.02	6.19	8.06	2.63	2.53
P_2O_5	0.35	0.31	0.76	0.30	0.26	0.32	0.62	0.52
LOI	1.19	0.99	2.08	2.54	0.96	1.49	2.42	2.05
Total	100.14	100.20	99.72	99.92	100.00	98.23	99.79	99.96
ppm								
Ag	<0.5	<0.5	<0.5	<0.5	<0.5	0.7	<0.5	<0.5
Ba	1502	456	644	3564	2280	5790	190	807
Bi	<0.4	<0.4	<0.4	<0.4	<0.4	3.8	<0.4	<0.4
Cs	1.8	1.6	<0.5	1.0	0.5	1.4	1.4	1.2
Cu	<10	146	51	385	ND	8240	ND	1020
Ga	19	20	21	18	21	20	19	20
Ge	1.2	1	0.8	<1	1.1	0.9	2.00	1.3
Hf	5.1	4.3	9.1	4.4	8.8	7.2	3.2	2.6
In	<0.2	<0.2	<0.2	<0.2	<0.2	<0.2	<0.2	<0.2
Nb	9	7	9	7	14	11	7	4
Ni	21	47	<20	<20	64	<20	48	74
Pb	6	6	30	<5	15	<5	6	<5
Rb	157	97	24	106	135	177	117	85
Sn	<1	1	1	<1	1	3	4	<1
Sr	403	269	207	399	295	310	129	325
Ta	0.5	0.4	1.0	0.3	1.0	0.7	0.2	0.1
Tb	0.6	0.5	1.2	0.5	0.9	0.8	1.7	0.8
Th	7.3	5.3	15.3	4.0	11.2	8.5	2.5	0.5
Tl	0.4	0.5	<0.1	0.2	0.3	0.5	0.2	0.3
U	1.9	6.9	3.2	1.7	3.4	4.8	3.9	0.8
V	116	143	46	139	134	128	215	235
W	<1	<1	<1	3	<1	2	<1	<1
Y	16	15	37	13	23	24	47	26
Zn	38	34	52	430	44	36	37	82
Zr	201	171	359	150	303	275	114	87
La	35.4	60.4	65.8	30.1	86.4	81.6	93.5	19.0
Ce	79.0	115.4	168.0	63.7	159.0	144.0	305.0	41.0
Pr	9.3	11.9	20.7	7.37	17.2	15.0	36.2	5.25
Nd	35.6	43.2	74.0	30.0	66.4	55.3	145.0	23.7
Sm	6.1	6.5	14.5	5.1	11.3	7.5	21.8	4.7
Eu	1.45	1.83	2.77	1.64	2.10	2.10	5.55	1.90
Gd	4.3	4.4	9.1	3.8	5.8	5.5	14.9	5.4
Dy	2.9	0.5	6.9	0.5	4.9	4.3	9.5	4.7
Ho	0.6	2.7	1.4	2.6	0.8	0.9	1.6	1.0
Er	1.6	1.5	3.5	1.4	2.1	2.5	4.8	2.9
Tm	0.22	0.21	0.45	0.20	0.33	0.34	0.66	0.37
Yb	1.4	1.3	3.0	1.3	2.1	2.2	4.0	2.4
Lu	0.22	0.21	0.49	0.20	0.30	0.34	0.54	0.38
Cr[a]	71	50	50	23	75	77	24	102
Co[a]	23	27	16	61	14	15	26	51
As[a]	2.0	4.2	3.4	2	2.0	1.8	5.8	3.0
Mo[a]	<1	46	<1	<1	<1	36.0	<1	<1
Sb[a]	<1	0.4	0.6	<2	<1	0.9	<1	0.5
Au[a] (ppb)	<2	<2	<2	<2	<2	193.0	4.0	6.0
Br[a]	3.9	<0.5	4.5	<1	6.3	7.2	<0.5	2.0
S[b] (wt%)	NA	NA	NA	NA	NA	0.936	NA	0.069

Major elements analysed with ICP and trace elements with ICP-MS

NA not available

[a] Analysed by INAA

[b] Analysed by XRF

alteration by Na_2O contents reaching 9.57 wt%. This is clearly being illustrated in the Na_2O versus K_2O plot which also shows that Cu is correlated with potassic alteration (Fig. 7a).

The metadolerites are characterised by a SiO_2 range between 35.8 and 50.78 wt%, a higher CaO content, up to 9.16 wt%, compared to the metaandesites, and significantly lower Zr content (36–117 ppm). The metadolerites show the greatest variation in TiO_2 with concentrations varying from 0.64 to 2.37 wt%.

Rare earth elements (REE)

Compared to the K-feldspar altered metaandesites, the albite altered metaandesites display a greater range in

Fig. 7 Whole-rock geochemistry plots of the host rocks to the Tjårrojåkka deposits. **a** Na_2O-K_2O plot showing inverse relationship and correlation of Cu-mineralised samples to potassic alteration. **b** REE patterns of representative rock samples. Chondrite normalised after Boynton (1984). **c** Metaandesites and metadolerites plotted on the igneous spectrum diagram after Hughes (1973). **d** Rock classification diagram after Winchester and Floyd (1977) revised by Pearce (1996)
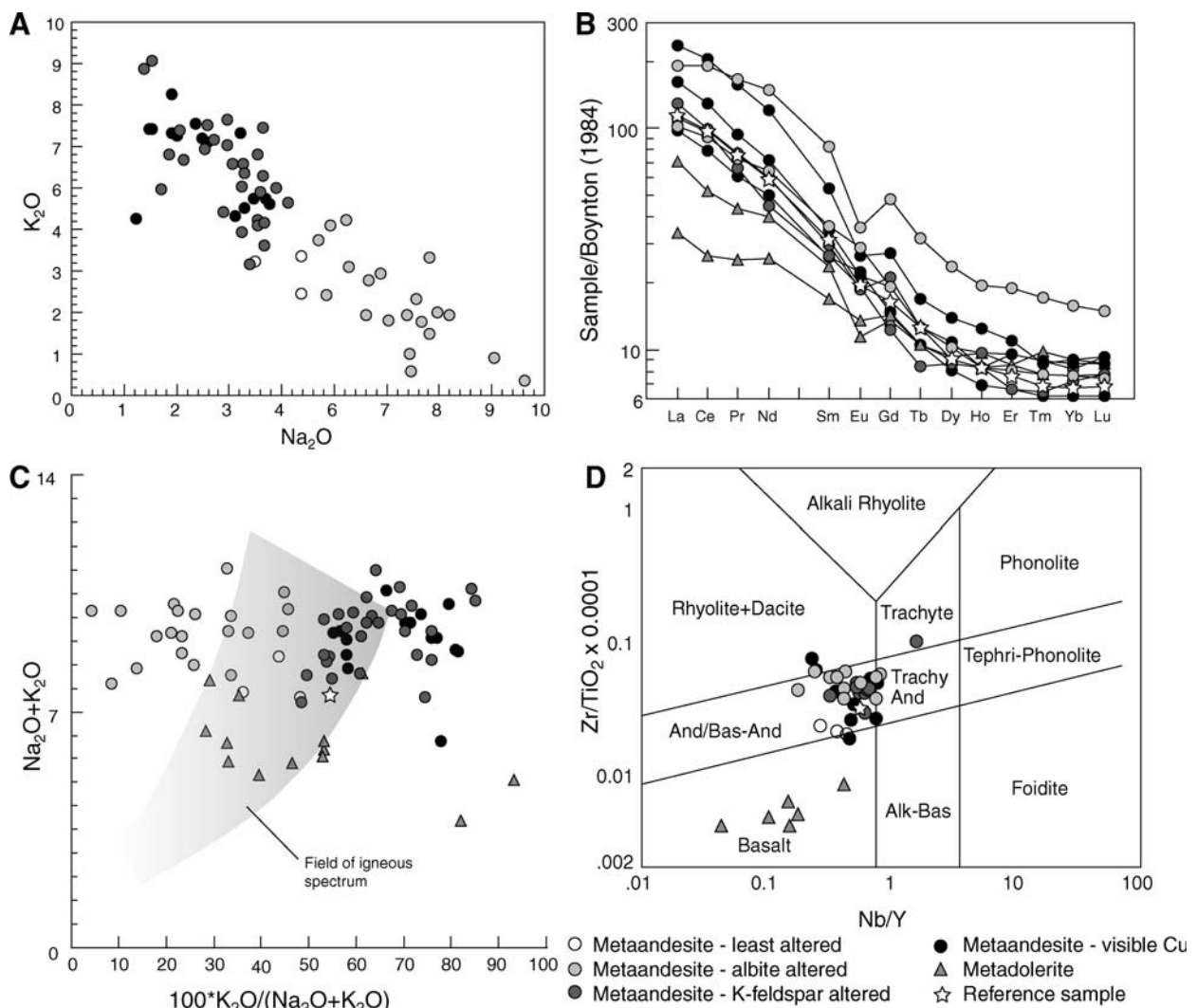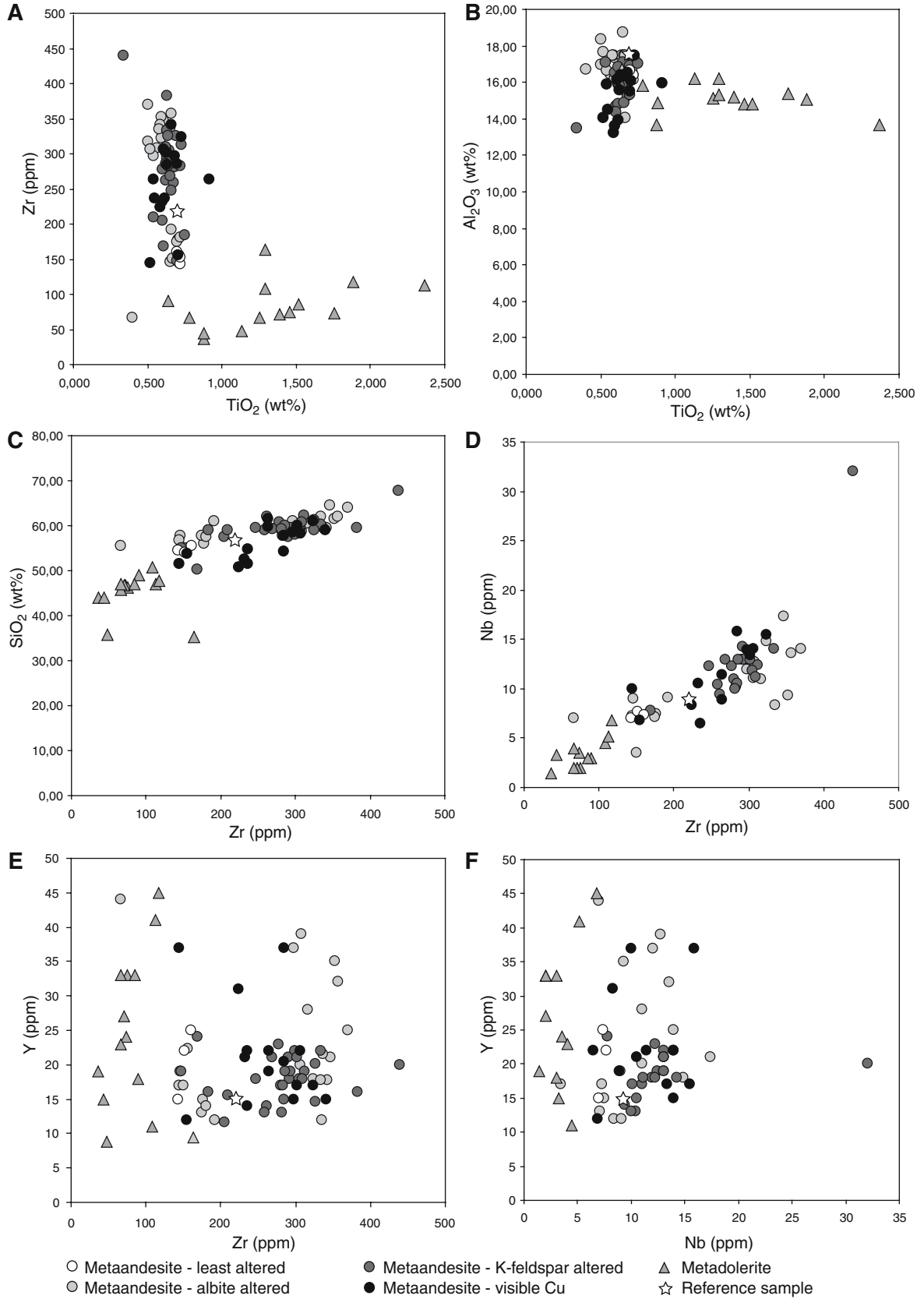
▶

Fig. 8 Immobile element plots for metaandesites and metadolerites at Tjårrojåkka

REE content. The La content of the K-feldspar altered samples varies between 26 and 86 ppm, with a mean of 51 ppm, while the La content of the albite altered samples varies between 15 and 208 ppm, with a mean of 58 ppm. The highest total REE content of the albite altered samples is comparable to the highest concentration observed in the mineralised samples.

The REE patterns of representative samples exhibiting different types of alteration and mineralisation, normalised after Boynton (1984), show LREE-enrichment and a negative Eu anomaly (Fig. 7b). The albite altered and Cu-mineralised samples show the greatest enrichment in REE compared to the least altered reference sample.

Element mobility during alteration and mineralisation

Element mobility was identified by plotting elements normally considered to be immobile (Al, Zr, Ti, Y, and

A — Zr (ppm) vs TiO₂ (wt%)

B — Al₂O₃ (wt%) vs TiO₂ (wt%)

C — SiO₂ (wt%) vs Zr (ppm)

D — Nb (ppm) vs Zr (ppm)

E — Y (ppm) vs Zr (ppm)

F — Y (ppm) vs Nb (ppm)

○ Metaandesite - least altered   ● Metaandesite - K-feldspar altered   ▲ Metadolerite

○ Metaandesite - albite altered   ● Metaandesite - visible Cu   ☆ Reference sample

Nb) against each other and other selected elements, and using isocon plots that compare concentrations of elements in altered relative to least altered samples (Grant 1986). The samples were divided into metadolerites and metaandesites, with the latter grouped as least altered, albite altered, K-feldspar altered and mineralised. The K-feldspar altered samples did not in most cases, show evidences of previous albitisation, which makes the comparison of element behaviour in the different alterations possible. The least altered sample used in the isocon plots was collected from an outcrop distal to the deposits and has a chemical composition similar to an unaltered Andean arc andesite (Raymond 1995).

A large number of samples plot outside the igneous spectrum in the diagram after Hughes (1973), and have higher total alkalis that expected, suggesting alkali mobility (Fig. 7c). In Fig. 7d the samples are plotted in the rock classification diagram Zr/TiO_2-Nb/Y after Winchester and Floyd (1977) (revised by Pearce [1996]), which shows that most samples retain andesitic and basaltic affinity even after metamorphism and intense hydrothermal alteration. Most of the samples affected by K-feldspar alteration cluster relatively well (with one exception), while the albite altered and mineralised samples show a greater spread.

The behaviour of elements normally considered immobile is illustrated in Fig. 8. The two clear trends that can be distinguished in the TiO_2-Zr plot indicate different origins of the intermediate and basic rocks and are in agreement with what has been observed in regional studies (Edfelt 2003). The roughly straight trends and clusters of Zr, TiO_2, Al_2O_3, and SiO_2, (Fig. 8a–c) suggest that these elements were, for the most part, conserved in the system and that the large variation of Zr in the andesites probably is a primary fractionation. Y, however, is more scattered and can be considered to have been mobile (Fig. 8e, f). The plot of Zr–Nb (Fig. 8d) show that albite altered and mineralised samples scatter most, while the K-feldspar altered are well clustered, which might indicate some degree of Nb mobility in these systems. Fig. 8f also demonstrates that Y was least mobile associated with K-feldspar alteration, but was mobile in the dolerites and related to albite alteration and mineralised samples. This also explains the spread of the dolerite samples in the classification diagram (Fig. 7d).

In the isocon diagrams TiO_2, Al_2O_3, SiO_2 and Zr lie very close to the ideal isocon for all three groups of samples (albite altered, K-feldspar altered, and mineralised), suggesting that they were relatively immobile in all systems (Fig. 9). However, in the K-feldspar altered samples Zr show a slight enrichment compared to the reference sample. Albite alteration caused significant addition of Na_2O and some addition of P_2O_5, resulting in the formation apatite, and a depletion of K_2O, MnO, and Fe_2O_3. In the isocon diagram for K-feldspar altered samples, K_2O, MnO, and P_2O_5 show the inverse relationship compared to the albite altered samples. K_2O, MnO, P_2O_5, and Fe_2O_3 have been added in the min-

▶

Fig. 9 Isocon diagrams for metaandesites showing elemental changes associated with alteration and mineralisation. Average values for groups of altered samples are compared with least altered reference sample; n(albite altered) = 22, n(K-feldspar altered) = 28, n(mineralised) = 15. Major oxides plotted in wt% and trace elements in ppm. For composition of reference sample see Fig. 7 and Table 3

eralised samples whilst CaO is depleted in all three groups compared to the reference sample.

Barium enrichment characterises K-feldspar altered and mineralised rocks and is greatest in the latter. A slight enrichment of Fe_2O_3 and V occurs in the mineralised samples, probably due to formation of magnetite. All REE elements are enriched in the altered and mineralised samples compared to the reference sample, which is in agreement with the results form the REE-patterns (cf. Fig. 7b). The greatest addition of REE is observed in the mineralised samples.

Mineral chemistry

Silicates

Representative chemical compositions of feldspars are shown in Table 4. Feldspars are among the most abundant alteration minerals in the two deposits and can be divided into three groups: potassium feldspar (Or > 90%), albite (Ab > 90), and plagioclase (An 75–45). Albitisation is restricted to the host rock surrounding the Tjårrojåkka-Fe deposit and the footwall of the Tjårrojåkka-Cu deposit, whereas K-feldspar alteration is locally developed in the Tjårrojåkka-Fe deposit associated with Cu-mineralisation and in the hanging wall of the Tjårrojåkka-Cu deposit. Plagioclase occurs in parts of the Tjårrojåkka-Fe deposit. The potassium feldspars have a varying content of Ba substituted for K, but there does not seem to be a systematic variation within individual grains. However, Cu-mineralised samples and pervasive K-feldspar alteration tend to be richer in Ba than non-mineralised samples and K-feldspar occurring in veins. Some samples from the apatite–iron occurrence contain more than 2 wt% BaO (Fig. 10) and can be considered as hyalophane (Deer et al. 1992).

Scapolite has a meionite ($Ca_4Al_6Si_6O_{24}CO_3$) content (Me = 100×Ca/(Ca + Na + K) between 30 and 55 (Fig. 11a). The Cl content varies between 0.9 and 2.9 wt% and CO_2 between 1.2 and 2.8 wt% while the F content is less than 0.2 wt% (Table 5). The SO_3 contents show wide variation from 0 to 1.5 wt%. The scapolite in the Tjårrojåkka-Fe deposit has higher Cl (2.3–2.9 wt%) and lower S content than samples from Tjårrojåkka-Cu deposit (Fig. 11b). Scapolite from unmineralised wall rock has a distinct character in being richer in CO_2 than scapolite related to mineralisation.

The composition of biotites, shown in Table 6, is between phlogopite/annite and eastonite. The Ti content varies from 1 to 3 wt% TiO_2, with the highest contents in biotite associated with the Tjårrojåkka-Cu deposit. The
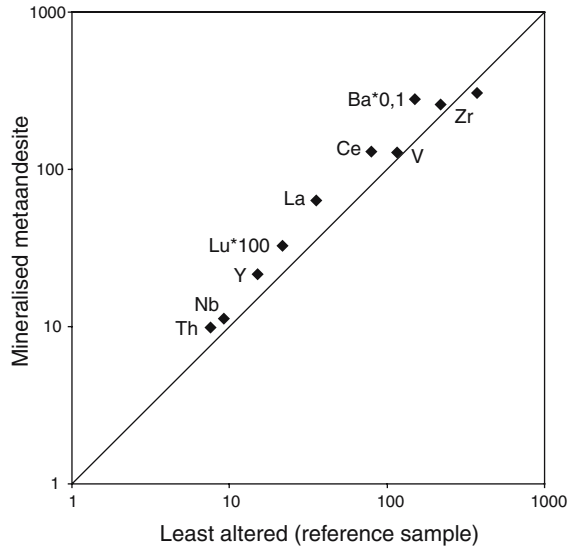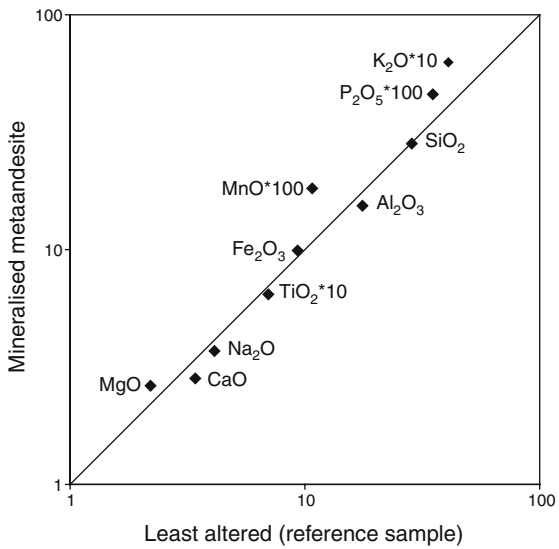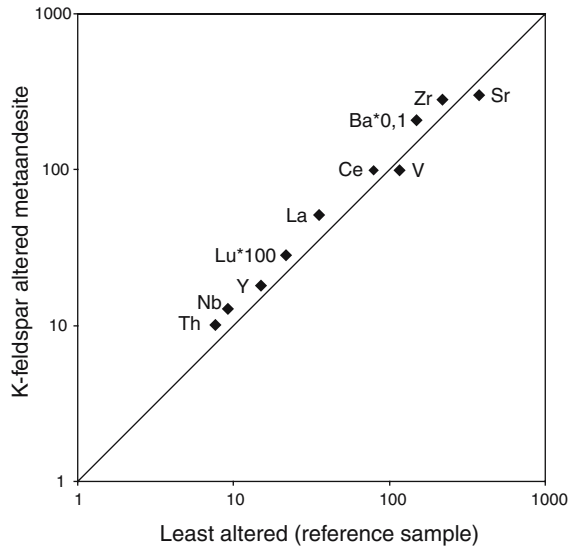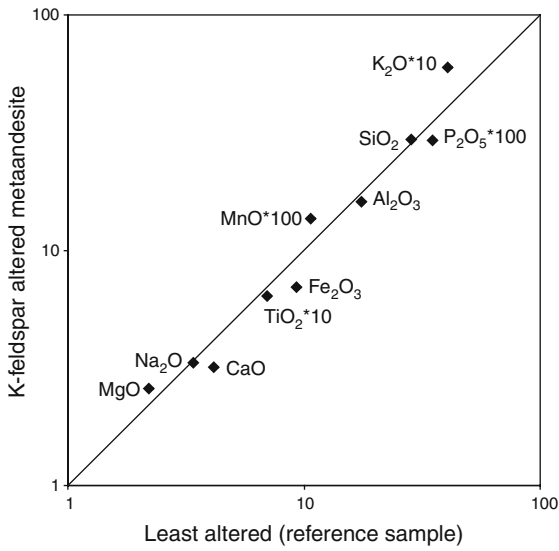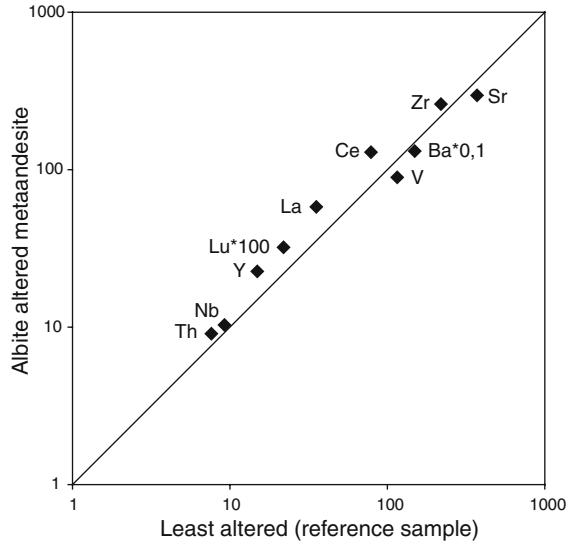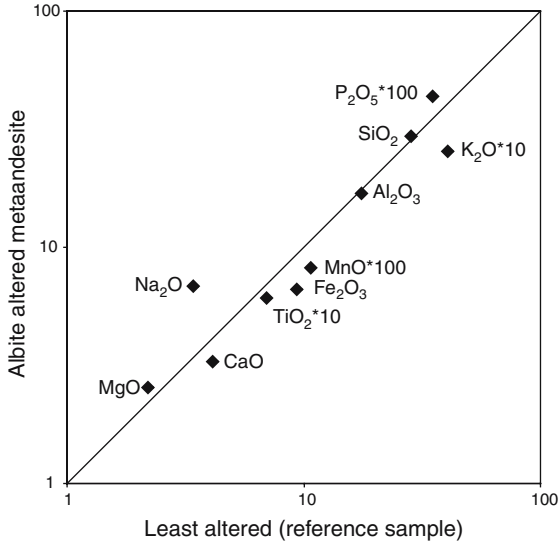
Table 4 Representative results of electron-microprobe analyses of feldspars

Sample	67306:250.61	74319:200.0	75316:75.10	71305:166.62	71305:392.4	67306:250.61	67306:279.0
Deposit	Tj–Fe	Tj–Cu	Tj–Cu	Tj–Cu	Tj–Cu	Tj–Fe	Tj–Fe
SiO_2	63.42	63.08	64.32	64.91	69.09	64.15	56.64
TiO_2	ND	ND	ND	0.02	ND	0.02	0.05
Al_2O_3	18.78	18.67	17.82	18.23	19.44	22.86	27.45
FeO^a	ND	0.05	0.04	0.09	ND	0.07	0.32
MgO	ND	ND	0.03	ND	0.02	ND	0.12
BaO	2.60	1.37	0.74	0.26	ND	ND	ND
CaO	ND	ND	ND	ND	0.05	4.00	8.90
Na_2O	1.22	1.09	0.61	0.20	11.24	9.38	6.42
K_2O	14.50	15.64	16.28	16.75	ND	0.13	0.18
Total	100.51	99.89	99.83	100.45	99.85	100.61	100.06
Or	79.17	86.43	92.35	97.35	0.14	0.96	1.17
Ab	6.65	6.01	3.45	1.15	99.39	69.45	41.42
An	0.00	0.00	0.00	0.00	0.47	29.59	57.40
Celsian	14.19	7.56	4.20	1.50	0.00	0.00	0.00
Number of cations on the basis of 32O							
Si	11.83	11.82	12.00	12.00	12.04	11.26	10.17
Ti	0.00	0.00	0.00	0.00	0.00	0.00	0.01
Al	4.13	4.12	3.92	3.97	3.99	4.73	5.81
Fe^{2+a}	0.00	0.01	0.01	0.01	0.00	0.01	0.05
Mg	0.00	0.00	0.01	0.00	0.01	0.00	0.03
Ba	0.19	0.10	0.05	0.02	0.00	0.00	0.00
Ca	0.00	0.00	0.00	0.00	0.01	0.75	1.71
Na	0.44	0.40	0.22	0.07	3.80	3.19	2.23
K	3.45	3.74	3.87	3.95	0.00	0.03	0.04

ND Not detected
[a]All Fe as Fe^{2+}
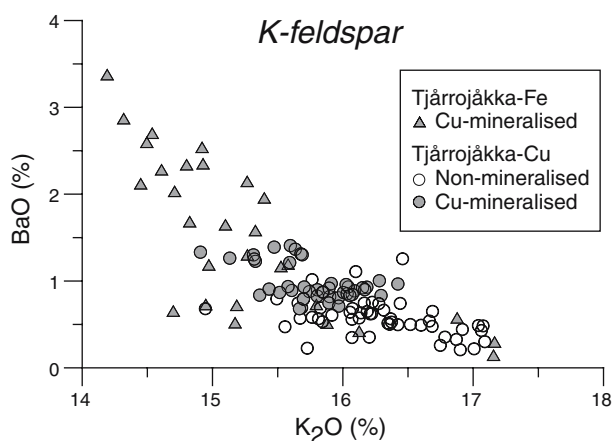
Fig. 10 Variation in BaO content in K-feldspar

Ba content is higher in Cu-mineralised samples than in non-mineralised samples. The amount of Cl varies between 0.2 and 0.5 wt% and F between 0 and 0.8 wt%. The biotites from the apatite–iron ore plot in two distinct groups with respect to the Mg/Fe and F contents (Fig. 12a). In, or close to the breccia, the Mg content is higher and the F content lower, than in the samples outside. The sample that shows the highest F values is also richest in Cl (0.5–0.6 wt%). The biotites from the Tjårrojåkka-Cu deposit show less variation in Mg/Fe ratio, but Cu-mineralised samples are generally more Mg-rich (Fig. 12a, b). In Fig. 12b three linear trends can be distinguished with the amount of Cl increasing with Fe.

The amphiboles in the Tjårrojåkka-Fe and -Cu deposits are Ca-rich and range from tschermakite to magnesio-hornblende to actinolite and tremolite (Table 7 and Fig. 13a). The most widespread types are tschermakite and Mg-hornblende occurring in the matrix, often together with pervasive K-feldspar alteration, or in fractures together with chalcopyrite or bornite. Actinolite is found in veins where it generally is paragenetically later the other amphiboles, in the breccia surrounding the apatite–iron body, and in the Tjårrojåkka-Cu deposit. Tremolite only occurs as veinlets in the massive magnetite ore in the Tjårrojåkka-Fe deposit. The amount of Cl in the amphiboles increases with the Fe content and is highest in the tschermakites (Fig. 13b). F is present in the amphiboles in the Tjårrojåkka-Cu deposit (0.1–0.2 F per formula unit) but it is below detection limit in the amphiboles from the Tjårrojåkka apatite–iron ore.

Chlorite, titanite, epidote and allanite are minor constituents among the rock-forming and hydrothermal alteration mineral assemblages and their chemistry will not be discussed in detail. Titanite is more common in the alteration assemblages in the copper deposit and contains between 0.2 and 1.2 wt% F, around 1–2 wt% Fe_2O_3 and traces of Ce. The Fe_2O_3 content in the epidote varies between 15.5 and 17.2 wt%. REE were not detected.

Apatite

The analysed apatites classify as fluor-apatites with F contents between 1.6 and 3.4 wt% (Table 8). The apatites in the copper occurrence have higher F than those
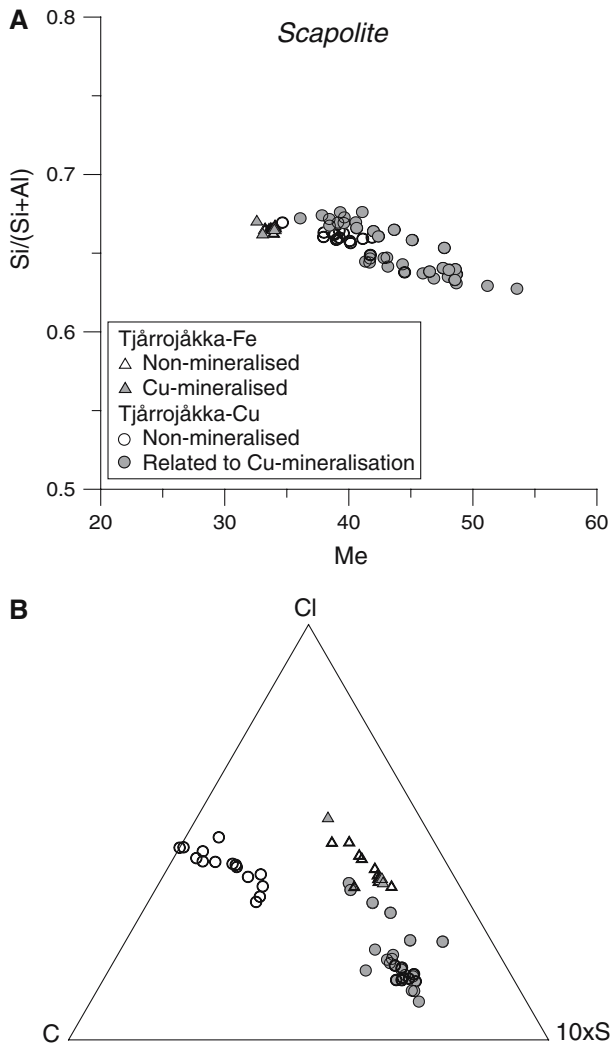
A

Scapolite

Si/(Si+Al)

Tjårrojåkka-Fe
△ Non-mineralised
▲ Cu-mineralised
Tjårrojåkka-Cu
○ Non-mineralised
● Related to Cu-mineralisation

Me

B

Cl

C   10xS

Fig. 11 Variation in scapolite composition. **a** Diagram showing variation in meionite (*Me*) content. $Me = 100 \times Ca/(Ca + Na + K)$. **b** Cl-C-S diagram. All atoms per formula unit

in the iron ore. Apatites from an unmineralised outcrop of metaandesite, located about 1 km WNW of the Tjårrojåkka deposits, are the most F-rich (Fig. 14).

The apatites in the massive magnetite ore in Tjårrojåkka-Fe are the most Cl-rich (0.9–1.6 wt%), with a few exceptions that show Cl values around 0.3 wt% probably due to zoning with the rims being Cl-poorer. The slightly high totals in the analyses may be a result of either the breakdown of the mineral under the electron beam or a calibration problem due to partial breakdown of the standards with time.

Sulphides and oxides

Representative analyses for sulphides (chalcopyrite, pyrite and bornite) and oxides (magnetite and hematite) are presented in Table 9. The sulphides do not show large compositional variations between the two deposits. In a few samples, chalcopyrite shows traces of Se, Ag and Au and some pyrites associated with the

Tjårrojåkka-Cu deposit have significant Co contents of up to 1.8 wt%. Cr, Mn, Ni, Sb, Te, Hg, Pb, and Bi were also analysed, but were below detection limits.

The V_2O_5 content in magnetite and hematite range from 0.1 to 0.9 wt%, with the highest values in hematite from the Tjårrojåkka-Cu deposit. Mn, Co, and Ni were also detected in some of the samples, but are generally below the detection limit. There do not seem to be any systematic variations in minor element compositions of iron oxides (Al, Ti, V, and Mn), except for Cr which is slightly enriched in magnetite associated with copper sulphides.

Discussion

Element mobilisation and chemical variations

Element mobilisation and redistribution is common during hydrothermal alteration, however, in terrains that have been subject to extensive regional alteration, metamorphism and/or metasomatism the quantification of element mobility is difficult. In the case of the Tjårrojåkka occurrences, the degree of element mobility and transport is best illustrated by considering the geochemical systematics of the metaandesitic rocks. Thirtynine percent of the samples plot outside the igneous spectrum in the diagram after Hughes (1973) as a result of potassic and sodic alteration (cf. Fig. 7c). The data show that the albite altered metaandesites (mainly in the footwall of the Tjårrojåkka-Cu deposit and the host rock of the Tjårrojåkka-Fe deposit) have been subject to a relative enrichment in Na, while the hanging wall of the Tjårrojåkka-Cu and the copper mineralised zones are characterised by a relative enrichment in K.

The distributions of both the major, minor and trace elements suggest that the degree of mobility within the K-enriched and Na-enriched samples is systematically different. This is particularly well illustrated by the distribution of Na_2O, K_2O, P_2O_5, Ba, Y, and REE. Albite altered and mineralised samples scatter in Y and REE plots, indicating that the elements were mobile in these systems, while the K-feldspar altered samples cluster. The variation of Y in the dolerites could be due to the intense scapolite alteration breaking down primary mafic minerals.

Mobility of Zr, Ti and REE during hydrothermal processes has been noted by many authors, including Gieré (1990) and Rubin et al. (1993), in fluids where P, F, and K and/or Na were important components along with high activity of CO_2. However, the variation of Zr and Ti in the andesites is most probably a result of primary fractionation although Zr shows a slight enrichment in the K-feldspar altered samples and hydrothermal zircons and titanites have been observed. On the other hand, the enrichment of REEs in altered and mineralised samples, relative to least altered, and the presence of allanite and late REE-carbonates indicate that REE were mobile at Tjårrojåkka.

Table 5 Representative results of electron-microprobe analyses of scapolite

Sample Deposit	67306: 279.0 Tj–Fe	75311: 255.96 Tj–Cu	75311: 13.0 Tj–Cu	71305: 392.40 Tj–Cu	73311: 91.40 Tj–Cu	75316: 226.49 Tj–Cu
SiO_2	54.43	55.29	53.72	53.39	51.78	50.80
Al_2O_3	23.20	23.37	23.45	22.84	23.95	24.30
FeO^a	0.28	0.18	ND	0.08	0.12	0.13
CaO	8.46	9.03	9.72	10.73	11.23	12.51
Na_2O	8.82	7.53	8.32	6.94	7.71	7.01
K_2O	0.89	0.70	0.69	1.08	0.75	0.69
Cl	2.66	2.60	1.91	1.96	1.55	1.29
F	ND	ND	ND	0.07	ND	ND
SO_3	0.39	NA	0.05	1.09	1.03	1.35
CO_2^b	1.48	1.84	2.59	1.73	2.40	2.36
Total	100.60	100.53	100.44	99.90	100.52	100.43
Cl=O	0.59	0.58	0.42	0.44	0.34	0.29
F=O	0.00	0.00	0.00	0.03	0.00	0.00
Total	100.01	99.95	100.01	99.43	100.17	100.14
Number of cations on the basis of 12(Si, Al)						
Si	7.99	8.01	7.92	7.98	7.77	7.67
Al	4.01	3.99	4.08	4.02	4.23	4.33
Fe^{2+a}	0.03	0.02	0.00	0.01	0.02	0.02
Ca	1.33	1.40	1.54	1.72	1.81	2.02
Na	2.51	2.11	2.38	2.01	2.24	2.05
K	0.17	0.13	0.13	0.21	0.14	0.13
Cl	0.66	0.64	0.48	0.50	0.39	0.33
F	0.00	0.00	0.00	0.03	0.00	0.00
S	0.04	0.00	0.01	0.12	0.12	0.15
C^b	0.29	0.36	0.52	0.35	0.49	0.48

NA Not available; *ND* not detected
[a]All Fe as Fe^{2+}
[b]CO_2 and C calculated by difference

Table 6 Representative results of electron-microprobe analyses of biotite

Sample Deposit	69304: 45.53 Tj–Fe	71305: 449.15 Tj–Cu	74319: 200.0 Tj–Cu	75311: 255.96 Tj–Cu	73311: 91.40 Tj–Cu	67306: 250.61 Tj–Fe
SiO_2	34.25	36.65	36.54	37.12	36.52	37.98
TiO_2	2.03	2.40	2.88	2.73	2.10	0.99
Al_2O_3	17.48	16.22	15.35	13.12	14.10	14.55
FeO^a	22.24	18.45	16.60	17.85	17.14	15.37
MnO	0.21	0.43	0.67	0.55	0.80	0.15
MgO	8.35	11.47	13.18	13.91	14.23	16.18
CaO	ND	ND	ND	0.10	ND	0.04
BaO	0.07	0.06	0.20	0.11	0.16	0.21
K_2O	9.89	9.80	10.00	9.79	9.62	9.71
Na_2O	0.17	0.15	0.09	0.08	0.04	0.07
F	0.77	0.18	0.32	0.33	0.73	0.42
Cl	0.58	0.56	0.19	0.44	0.30	0.50
H_2O^b	3.34	3.73	3.77	3.67	3.53	3.69
Total	99.37	100.08	99.78	99.80	99.28	99.87
Cl=O	0.04	0.03	0.01	0.03	0.02	0.03
F=O	0.16	0.04	0.06	0.07	0.15	0.08
Total	99.17	100.02	99.71	99.70	99.11	99.76
Number of cations on the basis of 22O						
Si	5.38	5.56	5.54	5.67	5.59	5.70
Ti	0.24	0.27	0.33	0.31	0.24	0.11
Al	3.23	2.90	2.74	2.36	2.55	2.57
Fe^{2+a}	2.92	2.34	2.10	2.28	2.20	1.93
Mn	0.03	0.06	0.09	0.07	0.10	0.02
Mg	1.95	2.60	2.98	3.16	3.25	3.62
Ca	0.00	0.00	0.00	0.02	0.00	0.01
Ba	0.00	0.00	0.01	0.01	0.01	0.01
K	1.98	1.90	1.93	1.91	1.88	1.86
Na	0.05	0.04	0.03	0.02	0.01	0.02
F	0.38	0.09	0.15	0.16	0.35	0.20

Table 6 (Contd.)

Sample Deposit	69,304: 45.53 Tj–Fe	71,305: 449.15 Tj–Cu	74,319: 200.0 Tj–Cu	75,311: 255.96 Tj–Cu	73,311: 91.40 Tj–Cu	67,306: 250.61 Tj–Fe
Cl	0.16	0.14	0.05	0.11	0.08	0.13
OH[b]	3.46	3.77	3.80	3.72	3.57	3.67

ND Not detected
[a]All Fe as Fe^{2+}
[b]OH and H_2O calculated by difference

Alteration paragenesis and the evolution of fluid chemistry

Similarity in alteration minerals and paragenesis may partly be a product of the common host rock to the

Fig. 12 Diagrams showing compositional variation in biotite. **a** Plot of F against $Mg/(Mg+Fe^{2+})$. **b** Plot of Cl against $Mg/(Mg+Fe^{2+})$

Tjårrojåkka-Fe and Tjårrojåkka-Cu occurrences, but is also an indication of similarities in fluid compositions and depositional conditions. Ba, Cl, F and S are elements enriched in the alteration minerals in the Tjårrojåkka occurrences and can be used as indicators of the nature of the hydrothermal fluids. Variation in the content of these elements in K-feldspar, scapolite, apatite, biotite and amphibole clearly suggests differences in the physical and/or chemical environment during alteration and mineralisation in the two deposits.

Barium feldspars commonly occur associated with manganese deposits (Deer et al. 1992), but have also been noted in, for example, the galena deposit at Korsnäs (Mäkipää 1976) and the Pikkuharju Cu–Zn mineralisation (Lahtinen and Johanson 1987) in Finland, the Rosh Pinah Pb–Zn deposit in Namibia (Page and Watson 1976), and the Ernest Henry IOCG-deposit in Australia (Mark et al. 2000). At Tjårrojåkka the Ba content in K-feldspar varies between the two deposits. In Tjårrojåkka-Fe deposit K-feldspar with a celsian component ($BaAl_2Si_2O_8$) occurs in the Cu-mineralised breccia surrounding the massive magnetite body indicating a high Ba/K ratio in the hydrothermal fluids responsible for this K-feldspar alteration. The amount of Ba in K-feldspar is lower in samples from the Tjårrojåkka-Cu deposit and lowest in the non-mineralised samples.

Scapolite is in some districts a common mineral in metamorphic and metsomatic rocks and can be used as an indicator of volatile activities and the Cl content of the fluid salinity (e.g. Shaw 1960; Vanko and Bishop 1982). The occurrence of marialite ($Na_4Al_3Si_9O_{24}Cl$)-rich scapolite indicates high activities of NaCl in the rock or fluid (Orville 1975) and regional occurrences of scapolite rich in Cl possibly indicate the presence of metamorphosed evaporitic sequences (Ellis 1978). The scapolite at Tjårrojåkka shows a trend with more Cl-rich varieties around the magnetite body trending towards higher SO_3- and CO_2-contents in the Tjårrojåkka-Cu deposit. The same compositional variation has been observed in the Malmberget apatite–iron ore (Fig. 1) where the scapolite is Cl-rich (3.8 wt%) and in the nearby Nautanen Cu–Au mineralisation (Fig. 1) scapolite is dominated by SO_3 and CO_2 (Frietsch et al. 1997). At Tjårrojåkka the scapolite most distal to the copper deposit is more CO_2-rich and SO_3-poor than scapolite from the mineralised part, and can hence be interpreted as having formed from a SO_3-depleted hydrothermal fluid.

Apatite is a common mineral in the Tjårrojåkka occurrences and since the three solid-solution end-
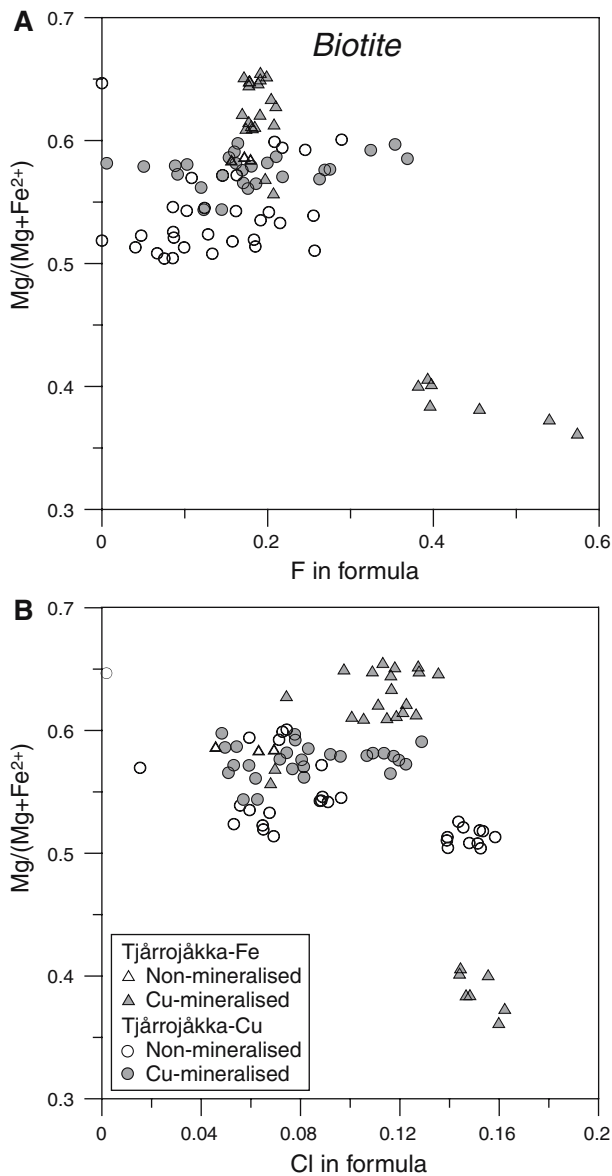
Table 7 Representative results of electron-microprobe analyses of amphiboles

Sample	73311: 91.40	68313: 263.75	71305: 199.46	71305:166.62	68313: 182.80
Ampibole	Tschermakite	Mg-hornblende	Mg-hornblende	Actinolite	Tremolite
Deposit	Tj–Cu	Tj–Fe	Tj–Cu	Tj–Cu	Tj–Fe
SiO_2	40.75	43.70	50.06	53.76	57.23
TiO_2	0.89	0.34	0.43	0.06	ND
Al_2O_3	10.27	8.98	4.84	2.18	0.38
Cr_2O_3	ND	0.04	0.03	0.02	0.05
Fe_2O_3 [a]	7.17	6.64	3.71	2.43	0.47
FeO[a]	13.16	11.10	10.72	9.67	3.55
MnO	1.17	0.30	0.67	0.74	0.05
MgO	9.31	11.69	14.23	16.06	22.21
CaO	11.62	11.99	12.20	12.56	13.70
Na_2O	1.56	1.26	0.94	0.33	0.13
K_2O	1.73	1.14	0.52	0.19	0.02
Cl	0.61	0.51	0.17	0.05	0.02
F	0.22	ND	ND	0.10	ND
H_2O[b]	1.70	1.88	1.87	2.03	2.17
Total	100.16	99.58	100.37	100.20	99.99
Cl=O	0.14	0.11	0.04	0.01	0.00
F=O	0.09	0.00	0.00	0.04	0.00
Total	99.93	99.47	100.34	100.14	99.99
Number of cations on the basis of 23O					
Si	6.25	6.56	7.26	7.69	7.90
Ti	0.10	0.04	0.05	0.01	0.00
Al	1.86	1.59	0.83	0.37	0.06
Fe^{3+a}	0.83	0.75	0.40	0.26	0.05
Fe^{2+a}	1.69	1.39	1.30	1.16	0.41
Mn	0.15	0.04	0.08	0.09	0.01
Mg	2.13	2.62	3.08	3.42	4.57
Cr	0.00	0.00	0.00	0.00	0.01
Ca	1.91	1.93	1.90	1.93	2.02
Na	0.46	0.37	0.26	0.09	0.03
K	0.34	0.22	0.10	0.03	0.00
Cl	0.16	0.13	0.04	0.01	0.00
F	0.11	0.00	0.14	0.05	0.00
OH[b]	1.74	1.87	1.82	1.94	2.00

ND Not detected
[a]Fe^{2+} and Fe^{3+} calculated using the method of Droop (1987) assuming 13 cations and 23(O,OH,F,Cl)
[b]Calculated assuming the (Cl,F,OH) site is filled

members constitute Cl-, F- and OH-apatites, these elements can be used as indicators of the composition of the hydrothermal fluids (Korzhinskiy 1982). Korzhinskiy (1982) also showed that the Cl/F ratio in apatite increases with temperature and that the pressure effects are negligible. The apatites analysed from an outcrop sample, located approximately one km WNW of the Tjårrojåkka deposits, have the highest F while those clearly related to the mineralising processes from the copper deposit are more Cl-rich. The outcrop apatites are clearly distinct from the apatites from the deposits and imply lower Cl activities during formation, reflecting either primary magmatic conditions or subsequent metamorphism of apatite in the presence of relatively low salinity fluids. Compared to apatite from the Kiirunavaara apatite–magnetite ore (Harlov et al. 2002) the apatites at Tjårrojåkka are richer in Cl and H_2O and poorer in F. La and Ce are generally lower while Nd shows similar values to the apatites in Kiirunavaara.

The interpretation of the halogen contents of silicate minerals is complicated by crystal chemical effects between the hydroxyl site and cation sites within the minerals, generally termed the Fe–F avoidance principle (e.g. Ekström 1972; Rosenberg and Foit 1977). The halogen composition of biotite (assuming no post-crystallisation re-equilibration) will be a function of the Mg:Fe ratio of the biotite as well as P-T conditions at the time of crystallisation, and the fluid chemistry (Zhu and Sverjensky 1991; Munoz 1984). Biotites from different parts of the systems do not show great variation in chemistry, except biotite from a distal part of the iron ore that differs from the others in being the most Fe-rich and showing the highest content of F. However, in a plot of Cl against $Mg/(Mg + Fe^{2+})$ (Fig. 8b), three linear trends can be distinguished originating from differences in temperature or salinity of the fluids, or representing different generations of biotite.

Previous studies have also suggested that the F and Cl contents of amphiboles are influenced by mineral structure and crystal chemistry (including the Fe–F and Mg–Cl avoidance effects) as well as the P-T conditions and halogen activity in the co-existing fluid (e.g. Oberti et al. 1993). All amphiboles at Tjårrojåkka are Ca-rich with the highest F content in the amphiboles in the Tjårro-
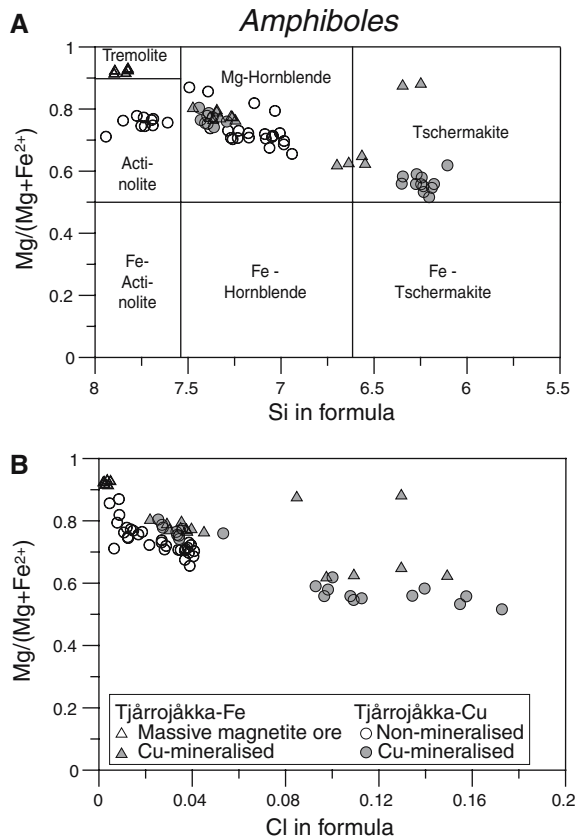
Fig. 13 Composition of amphiboles (cf. Table 7). **a** Classification of amphibole composition after Leake et al. (1997). **b** Variation in Cl content in amphiboles

jåkka-Cu deposit, and the highest Cl in the tschermakites. Oberti et al. (1993) showed that an increase in Cl content would require increasing Fe^{2+}, K, and Al which is consistent with the trends in the amphiboles from Tjårrojåkka. A more extensive interpretation of fluid composition from halogen chemistry in biotite, amphiboles and apatite would, however, require temperature and pressure data, which are currently not available.

Magnetite and hematite have similar geochemistry to magnetite from Kiirunavaara and El Laco in Chile (Nyström and Henríquez 1994) in being rich in V (average 2,860 ppm) and low in Ti (average 240 ppm) and Cr (average 340 ppm).

The fact that late REE-carbonates occur in the footwall of the copper deposit and that allanite rims on epidote are common indicate late infiltration of REE enriched fluids. Previous studies have shown that allanite and apatite may form as replacement products of monazite during hydrothermal alteration (Finger et al. 1998; Wing et al. 2003), which could explain the low content of REE in apatite (cf. Table 8) and the absence of monazite. Another possibility could be REE leaching from apatite during late stage alteration and metamorphism, which has been suggested to account for REE depleted apatite rims and the development of late stage monazite and allanite in the Kiirunavaara magnetite body (Harlov et al. 2002).

Overall, the alteration minerals (K-feldspar, scapolite, and apatite) related to the Tjårrojåkka apatite–iron ore are more Cl- and Ba-rich compared to the alteration minerals in the copper deposit that have higher contents of F and SO_3. Higher Ba in K-feldspar near the iron deposit could reflect lower fluid sulphate concentrations associated with a high Ba/K ratio, which is supported by higher Ba contents in whole-rock analyses of K-feldspar altered samples from Tjårrojåkka-Fe. The presence of in scapolite and the existence of minor barite and late hematite in the copper deposit point towards more oxidising conditions during the formation of the Tjårrojåkka copper deposit.

The mineral chemical and paragenetic results can be interpreted in two ways; either (a) there were two different hydrothermal systems; one reduced fluid with a high Ba/K ratio, high salinity and low sulphate concentration forming the Tjårrojåkka-Fe deposit, and another one more oxidised and $F-SO_4-CO_2$-rich forming the Tjårrojåkka-Cu deposit, or (b) there was one evolving system. An evolving system would require lowering of Cl contents of the fluid, which could be achieved either by fluid mixing or by loss of Cl to minerals, with the latter being a common feature in Cu–Au deposits in the Cloncurry district, Australia (Baker 1998). There, the loss of Cl from the fluids gave rise to hornblende and biotites with Cl contents up to 3.5 wt% and other Cl-bearing phases such as scapolite and apatite. However, at Tjårrojåkka the Cl content in the biotites and amphiboles is much lower (< 0.6 wt%), but scapolite and apatite in the apatite iron-body are more Cl-rich than in the copper deposit and could have influenced the reduction of salinity. Some preliminary fluid inclusion work on the Tjårrojåkka occurrences indicates moderately to highly saline (15–32 eq.wt% $CaCl_2$ + NaCl) systems (Broman and Martinsson 2000; Edfelt et al. 2004), which is in accordance with data from other copper deposits in the region (Wanhainen et al. 2003; Broman and Martinsson 2000; Lindblom et al. 1996). Edfelt et al. (2004) also noted an increase in salinity and the appearance of carbonate daughter minerals going from the apatite-forming stage to the Cu-sulphide stage, with a likely cause being fluid mixing.

The Tjårrojåkka occurrences as IOCG type deposits

The Tjårrojåkka Fe-oxide Cu–Au occurrences share many characteristics (structural control, abundance of iron oxides, anomalous concentrations of REE, albite-scapolite-K-feldspar alteration) with deposits classified as IOCG-type (e.g. Hitzman et al. 1992; Marschik and Fontboté 2001; Porter 2001). The common spatial relationship between apatite–iron and copper ores has also been noted between more recent deposits of Fe-oxide Cu-Au-type in Cretaceous iron belt (Naslund et al. 2002) and Candelaria-Punta del Cobre deposits (Marschik and Fontboté 2001) in Chile, which show many similar features with the Tjårrojåkka occurrences.

Table 8 Representative results of electron-microprobe analyses of apatite

| Sample | 75311: 255.96 | 75316: 328.50 | 29IAE215 | 68313: 120.20 | 67306: 250.61 |
Deposit	Tj–Cu	Tj–Cu	Outcrop	Tj–Fe	Tj–Fe
CaO	56.13	55.81	56.28	55.43	54.98
MgO	ND	ND	ND	ND	ND
SrO	0.11	0.09	0.05	0.09	0.08
MnO	0.19	0.09	0.16	ND	ND
FeO[a]	ND	ND	0.07	ND	ND
La$_2$O$_3$	0.07	ND	ND	0.09	ND
Ce$_2$O$_3$	0.14	ND	0.08	0.15	0.09
Nd$_2$O$_3$	0.20	ND	0.09	0.16	0.09
P$_2$O$_5$	41.31	42.23	42.23	41.42	41.64
SO$_3$	0.12	0.08	0.05	0.11	0.10
Cl	0.84	0.37	0.09	1.57	0.99
F	2.09	2.41	3.29	1.54	1.96
H$_2$O[b]	0.76	0.75	0.37	0.84	0.79
Total	101.95	101.82	102.74	101.38	100.71
Cl=O	0.05	0.02	0.01	0.10	0.06
F=O	0.46	0.52	0.70	0.34	0.43
Total	101.43	101.27	102.04	100.94	100.21
Number of cations on the basis of 26(O,OH,F,Cl)					
Ca	9.89	9.73	9.59	9.85	9.74
Mg	0.00	0.00	0.00	0.00	0.00
Sr	0.01	0.01	0.00	0.01	0.01
Mn	0.03	0.01	0.02	0.00	0.00
Fe^{2+}[a]	0.00	0.00	0.01	0.00	0.01
La	0.00	0.00	0.00	0.01	0.00
Ce	0.01	0.00	0.00	0.01	0.01
Nd	0.01	0.00	0.01	0.01	0.01
P	5.75	5.82	5.68	5.81	5.83
Cl	0.23	0.10	0.02	0.44	0.28
F	1.09	1.24	1.66	0.81	1.02
OH[b]	0.68	0.66	0.32	0.75	0.70

ND Not detected
[a]All Fe as Fe^{2+}
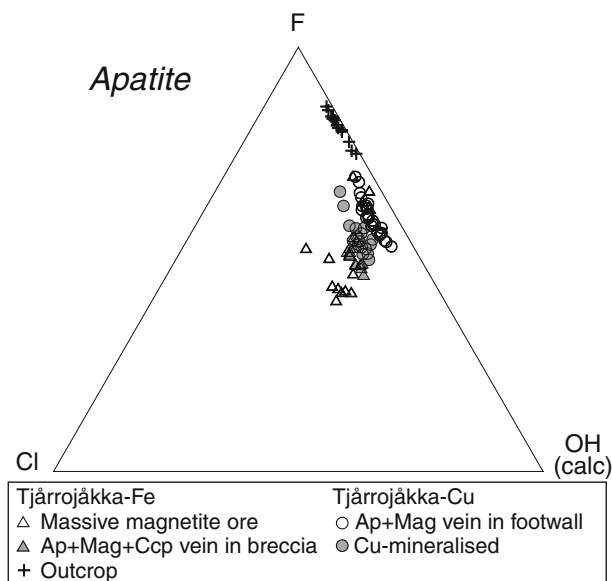[b]Calculated assuming the (Cl,F,OH) site is filled

Fig. 14 F-Cl-OH diagram showing compositional variation in apatite (atoms per formula unit)

The magnetite–apatite occurrence at Tjårrojåkka has similar characteristics to the Kiirunavaara apatite–iron ore with magnetite as almost the only iron oxide and a breccia developed along the wall rock contacts (Martinsson 2003). The Tjårrojåkka apatite–iron deposit differs from the Kiruna type apatite–iron ores in Norrbotten only in the higher sulphide content of the breccia surrounding the massive magnetite body. Both magmatic and hydrothermal replacement models have been suggested for the formation of the apatite–iron ores of Kiruna-type (e.g. Hitzman et al. 1992; Nyström and Henríquez 1994), but from the existing data it is not possible to prove either of these models for the Tjårrojåkka iron ore. However, the extensive hydrothermal alteration and veining around the massive magnetite body indicate that hydrothermal processes were definitely active at least at a later stage during the ore formation.

The Tjårrojåkka-Cu deposit might be related to this late stage hydrothermal activity and considered as a copper dominated end-member in the IOCG spectrum of deposits. It is characterised by strong sodic and

Table 9 Representative results of electron-microprobe analyses of sulphides and oxides

Mineral	Ccp	Ccp	Py	Bn	Ccp	Py	Bn
Sample	68313:166.4	69304:45.53	69304:45.53	68,313:29.0	75311:255.96	75311:255.96	75316:226.49
Deposit	Tj–Fe	Tj–Fe	Tj–Fe	Tj–Fe	Tj–Cu	Tj–Cu	Tj–Cu
Wt%							
S	34.82	34.63	52.89	25.27	37.19	50.02	26.19
Fe[a]	31.12	31.14	48.26	11.80	30.53	47.21	11.77
Co	ND	ND	0.05	ND	ND	1.67	ND
Cu	33.86	33.74	ND	62.96	31.97	ND	61.82
Zn	ND	0.15	ND	ND	0.04	ND	0.04
As	ND	ND	0.05	0.05	0.09	0.09	ND
Se	0.07	0.06	0.04	ND	0.02	0.03	ND
Mo	NA	NA	NA	NA	0.09	0.06	NA
Ag	ND	0.11	ND	ND	0.05	ND	ND
Au	0.19	ND	ND	ND	ND	ND	ND
Total	100.06	99.82	101.29	100.07	99.99	99.08	99.82

Mineral	Mag	Mag	Mag	Hem	Hem	Mag	Mag
Sample	68313:166.4	69304:218.16	68313:263.75	75316:328.50	75316:226.49	74319:335.50	75316:328.50
Deposit	Tj–Fe	Tj–Fe	Tj–Fe	Tj–Cu	Tj–Cu	Tj–Cu	Tj–Cu
V_2O_5	0.34	0.55	0.47	0.37	0.92	0.42	0.56
SiO_2	0.03	0.02	0.04	0.02	0.05	NA	0.05
TiO_2	0.03	ND	ND	ND	0.03	0.13	ND
Al_2O_3	0.22	0.12	0.04	0.04	0.04	0.06	0.03
Cr_2O_3	ND	ND	0.04	ND	0.07	NA	0.04
Fe_2O_3	52.06	51.99	52.19	99.41	97.21	52.11	52.11
FeO	46.96	46.90	47.08	[b]	[b]	47.01	47.01
MnO	0.046	ND	ND	0.07	0.05	0.13	0.10
MgO	ND	0.02	ND	ND	ND	NA	ND
ZnO	ND	ND	ND	0.05	ND	0.05	ND
NiO	ND	0.16	ND	0.05	ND	ND	ND
CaO	ND	0.03	ND	NA	NA	0.09	NA
Total	99.69	99.79	99.86	100.00	98.36	100.00	99.90

ND not detected; *NA* not available. *Ccp* chalcopyrite; *Py* pyrite; *Bn* bornite; *Mag* magnetite; *Hem* hematite
[a]Fe as Fe^{2+}
[b]All Fe as Fe^{3+}

potassic alteration comparable to those surrounding the apatite–iron ore, but show a stronger structural control. The presence of metadolerites in the mineralised zone in the Tjårrojåkka-Cu deposit could also have played and important role for mineralisation as pathways for the fluids.

Conclusions

The Tjårrojåkka occurrences can be considered as belonging to the IOCG-group of deposits representing two "end-members" of the class, with a spatial and possibly also genetic relationship. The Tjårrojåkka apatite–iron deposit has the typical characteristics of the Kiruna-type iron ores, except the high concentrations of sulphides in the surrounding ore breccia. The Tjårrojåkka-Cu occurrence is similar to epigenetic copper deposits in the region and other Fe-oxide Cu–Au deposits elsewhere in the world (e.g. Chile).

The whole-rock geochemistry indicates enrichment of alkalis related to mineralisation due to the formation of albite and K-feldspar. There was enrichment in Na and P and depletion of K, Ba, and Mn related to albitisation, with the inverse relationship of these elements associated with K-feldspar alteration. Fe and V show depletion in the altered zones and addition in mineralised samples. REE were enriched in the system, with the greatest addition related to mineralisation. Y mobility was associated with albite alteration and copper mineralisation.

Several generations and overlapping hydrothermal alteration stages indicate a long, complex history of fluid activity related to the formation of the Tjårrojåkka deposits. The two occurrences at Tjårrojåkka show a similar evolution in alteration paragenesis and mineralogy, but with more oxidising, CO_2-, F-, and -rich fluids related to copper deposit, in contrast to the Tjårrojåkka-Fe deposit where the fluids were more reduced with a higher salinity and Ba/K ratio. This might reflect one evolving system forming both occurrences, with the copper deposit representing slightly later products, but without geochronological data and more detailed fluid inclusion and isotopic studies we cannot rule out formation by two unrelated mineralising events.

was carried out at the Marie Curie ACCORD (Analytical and Computational Centre for Ore Deposits) Ph.D. training site at the Natural History Museum, London. We would like to thank John Spratt, Anton Kearsley and Terry Greenwood for their assistance with the analyses. Jan-Anders Perdahl, Roger Skirrow, and Patrick Williams are thanked for their thoughtful reviews and valuable comments, which substantially improved the manuscript.

Appendix

Descriptions of drill core samples analysed for mineral chemistry

Sample no.	Profile	Occurrence	Description
29IAE215	Outcrop	Outcrop	Andesite, Kfs altered
67306:250.61	400W	Tj–Fe	Mag + Ap vein with Ccp + Py in breccia, Kfs altered
67306:279.0	400W	Tj–Fe	Scp + Bt alteration with disseminated Mag + Ap
68313:120.20	400W	Tj–Fe	Massive Mag with Ap + Am + Carb fracture infill
68313:166.40	400W	Tj–Fe	Massive Mag with Ap + Carb + Ccp + Au fracture infill
68313:182.80	400W	Tj–Fe	Massive Mag with Hem vein and Ap + Am + Carb fracture infill
68313:263.75	400W	Tj–Fe	Mag + Am vein with disseminated Ccp in breccia, Kfs altered
68313:29.0	400W	Tj–Fe	Disseminated Ccp + Bn + Mag + Ap in Kfs altered rock
68313:76.60	400W	Tj–Fe	Ccp + Py + Mag in Am + Qtz vein in Kfs + Bt altered rock with disseminated Ccp + Py + Mag
69304:218.16	400W	Tj–Fe	Ccp + Py + Mag in Pl + Bt altered rock
69304:45.53	400W	Tj–Fe	Disseminated Ccp + Py + Mag in Kfs + Bt altered rock
71305:166.62	320E	Tj–Cu	Am + Kfs + Ttn vein cutting Mag + Ap alteration in footwall
71305:199.46	320E	Tj–Cu	Ab, Scp and Kfs altered rock in hanging wall
71305:392.40	320E	Tj–Cu	Kfs and Bt-altered hanging wall
71305:449.15	320E	Tj–Cu	Kfs and Bt-altered hanging wall
73311:91.40	320E	Tj–Cu	Ccp + Py + Mag in veinlets of Am, mineralised zone

Appendix (Contd.)

74319:200.0	600E	Tj–Cu	Ccp + Bn disseminated in Kfs, Bt, Am-altered rock, mineralised zone
74319:335.50	600E	Tj–Cu	Mag + Ap + Am vein with Ccp in footwall
75311:13.0	320E	Tj–Cu	Am + Ep + Qtz vein in Kfs and Scp-altered hanging wall
75311:255.96	320E	Tj–Cu	Ccp + Py + Mag in Am veinlets, mineralised zone
75316:226.49	120E	Tj–Cu	Scp + Bt-altered hanging wall
75316:328.50	120E	Tj–Cu	Mag + Ap + Am vein in footwall
75316:75.10	120E	Tj–Cu	Kfs and Am altered rock in hanging wall

Am amphibole; *Ap* apatite; *Bt* biotite; *Carb* carbonate; *Ep* epidote; *Kfs* K-feldspar; *Pl* plagioclase; *Qtz* quartz; *Scp* scapolite; *Ttn* titanite; *Au* gold; *Bn* bornite; *Ccp* chalcopyrite; *Hem* hematite; *Mag* magnetite; *Py* pyrite

References

Allen RL, Martinsson O, Weihed P (2004) Sveconfennian ore-forming environments: volcanic-associated Zn-Cu-Au-Ag, intrusion-associated Cu-Au, sediment-hosted Pb-Zn, and magnetite-apatite deposits of northern Sweden. In: Thompson TB (ed) Society of Economic Geologists Guidebook Series 33. CD-ROM ISSN 1547–3104

Baker T (1998) Alteration, mineralization, and fluid evolution at the Eloise Cu-Au deposit, Cloncurry District, Northwest Queensland, Australia. Econ Geol 93:1213–1236

Bergman S, Kübler L, Martinsson O (2001) Description of regional geological and geophysical maps of northern Norrbotten County (east of the Caledonian orogen). Geological Survey of Sweden, Ba 56, p 110

Billström K, Martinsson O (2000) Links between epigenetic Cu-Au mineralizations and magmatism/deformation in the Norrbotten county, Sweden. In: Weihed P, Martinsson O (eds) Second annual GEODE-Fennoscandian shield field workshop on Palaeoproterozoic and Archaean greenstone belts and VMS districts in the Fennoscandian Shield. Luleå University of Technology, p 6

Boynton WV (1984) Cosmochemistry of the rare earth elements: meteorite studies. In: Henderson P (eds) Rare earth element geochemistry. Elsevier, Amsterdam, pp 63–114

Broman C, Martinsson O (2000) Fluid inclusions in epigenetic Fe-Cu-Au ores in northern Norrbotten. In: Weihed P, Martinsson O (eds) Second annual GEODE-Fennoscandian shield field workshop on Palaeoproterozoic and Archaean greenstone belts and VMS districts in the Fennoscandian Shield. Luleå University of Technology, p 7

Deer WA, Howie RA, Zussman J (1992) An introduction to the rock-forming minerals. Pearson Education Limited, Essex, p 696

Droop GTR (1987) A general equation for estimating Fe^{3+} concentrations in ferromagnesian silicates and oxides from microprobe analyses, using stoichiometric criteria. Mineral Mag 51:431–435

Edfelt Å (2003) Geology, alterations, and mineral chemistry of the Tjårrojåkka Fe-oxide Cu-Au occurrences, northern Sweden. Licentiate Thesis, Division of Ore Geology, Luleå University of Technology, ISSN: 1402–1757

Edfelt Å, Broman C, Martinsson O (2004) A preliminary fluid inclusion study of the Tjårrojåkka IOCG-occurrence, Kiruna area, northern Sweden. In: Mansfeld J (ed) The 26th nordic geological winter meeting. Uppsala, 6–9 January 2004, GFF 126, p 148

Edfelt Å, Martinsson O (2003) The Tjårrojåkka Fe-oxide Cu (-Au) occurrence, Kiruna area, northern Sweden. In: Eliopoulos DG et al (eds) Mineral Exploration and Sustainable Development. Athens, 24–28 August 2003. Millpress, pp 1069–1071

Edfelt Å, Martinsson O (2004) The Tjårrojåkka Fe-oxide and Cu-Au occurrences, northern Sweden—products of one ore-forming event? IAVCEI General Assembly 2004. Pucón, Chile, 14–19 November

Ekström M (1978) Mineralogisk karakteristik av kopparmineraliseringen vid Tjårrojåkka. Geological Survey of Sweden, BRAP 78002, p 13 (in Swedish)

Ekström TK (1972) The distribution of fluorine among some coexisting minerals. Contrib Mineral Petrol 34:192–200

Ellis DE (1978) Stability and phase equilibria of chloride and carbonate bearing scapolites at 750°C and 4000 bar. Geochim Cosmochim Acta 42:1271–1281

Ettner DC, Bjorlykke A, Andersen T (1993) Fluid evolution and Au-Cu genesis along a shear zone: a regional fluid inclusion study of shear zone-hosted alteration and gold and copper mineralization in the Kautokeino greenstone belt, Finnmark, Norway. J Geochem Exp 49:233–267

Finger F, Broska I, Roberts MP, Schermaier A (1998) Replacement of primary monazite by apatite-epidote coronas in an amphibolite facies granite gneiss from the eastern Alps. Am Mineral 83:248–258

Frietsch R (1966) Berggrund och malmer i Svappavaarafältet, norra Sverige. Geological Survey of Sweden, C 604, p 282 (in Swedish)

Frietsch R, Tuisku P, Martinsson O, Perdahl J-A (1997) Early Proterozoic Cu-(Au) and Fe ore deposits associated with regional Na-Cl metasomatism in northern Fennoscandia. Ore Geol Rev 12:1–34

Geijer P (1910) Igneous rocks and iron ores of Kiirunavaara, Luossavaara and Tuolluvaara. Scientific and practical researches in Lapland arranged by Luossavaara-Kiirunavaara Aktiebolag, p 278

Gieré R (1990) Hydrothermal mobility of Ti, Zr and REE: examples from the Bergell and Adamello contact aureoles (Italy). Terra Res 2:60–67

Grant JA (1986) The isocron diagram—a simple solution to gresens' equation for metasomatic alteration. Econ Geol 81:1976–1982

Grip E, Frietsch R (1973) Malm i Sverige 2. Almqvist & Wiksell, Stockholm, p 295 (in Swedish)

Harlov DE, Andersson UB, Forster H-J, Nyström JO, Dulski P, Broman C (2002) Apatite-monazite relations in the Kiirunavaara magnetite-apatite ore, northern Sweden. Chem Geol 191:47–72

Hitzman MW, Oreskes N, Einaudi MT (1992) Geological characteristics and tectonic setting of Proterozoic iron oxide (Cu-U-Au-REE) deposits. Precamb Res 58:241–287

Hughes CJ (1973) Spilites, keratophyres, and the igneous spectrum. Geol Mag 109:513–527

Korzhinskiy MA (1982) Apatite solid solutions as indicators of the fugacity of HCl and HF in hydrothermal fluids. Geochem Int 3:45–60

Lahtinen R, Johanson B (1987) Barium feldspar from Pukkiharju base-metal mineralisation, central Finland. Bull Geol Soc Finland 59:77–80

Leake BE, Woolley AR, Birch WD, Gilbert MC, Grice JD, Hawthorne FC, Kato A, Kisch HJ, Krivovichev VG, Linthout K, Laird J, Maresch WV, Nickel EH, Schumacher JC, Smith DC, Stephenson NCN, Whittaker EJW, Youzhi G (1997) Nomenclature of amphiboles: report of the subcommittee on amphiboles of the international mineralogical association commission on new minerals and mineral names. Mineral Mag 61:295–321

Lindblom S, Broman C, Martinsson O (1996) Magmatic-hydrothermal fluids in the Pahtohavare Cu-Au deposit in greenstone at Kiruna, Sweden. Miner Deposita 31:307–318

Lindskog LV (2001) Relationships between Fe-oxide Cu/Au depostis at Gruvberget—Kiruna district Northern Sweden. BSc Thesis. School of Earth Sciences, James Cook University, p 123

Lundberg B, Smellie JAT (1979) Painirova and Mertainen iron ores: two deposits of the Kiruna iron ore type in northern Sweden. Econ Geol 74:1131–1152

Mark G, Oliver NHS, Williams PJ, Valenta RK, Crookes RA (2000) The evolution of the Ernest Henry Fe-oxide-(Cu-Au) hydrothermal system. In: Porter TM (eds) Hydrothermal iron oxide copper-gold & related deposits: a global perspective. Australian Mineral Foundation, Adelaide, pp 123–136

Marschik R, Fontboté L (2001) The Candelaria-Punta del Cobre Iron Oxide Cu-Au(-Zn-Ag) Deposit, Chile. Econ Geol 96:1799–1826

Martinsson O (2000) Metallogeny of the northern Norrbotten Fe-Cu-Au-ore province. In: Weihed P, Martinsson O (eds) Second annual GEODE-Fennoscandian shield field workshop on Palaeoproterozoic and Archaean greenstone belts and VMS districts in the Fennoscandian Shield. Luleå University of Technology, pp 26–28

Martinsson O (2003) Characterisation of iron mineralisations of Kiruna type in the Kiruna area, northern Sweden. In: Eliopoulos DG et al (ed) Mineral exploration and sustainable development. Athens, 24–28 August 2003. Millpress, pp 1087–1090

Martinsson O, Perdahl J-A (1994) Different types of Paleoproterozoic mafic to felsic volcanism in northernmost Sweden: products of underplating and subduction. Terra Nova 6:11

Munoz JL (1984) F-OH and Cl-OH exchange in micas with applications to hydrothermal ore deposits. In: Bailey SW (ed) Micas. Mineralogical Society of America, pp 469–493

Mäkipää H (1976) Korsnäsin strontium-maasälvästä. MSc Thesis. Department of Geology, University of Helsinki, p 99 (in Finnish)

Naslund HR, Henríquez F, Nyström JO, Vivallo W, Dobbs FM (2002) Magmatic iron ores and associated mineralisation: examples from the Chilean High Andes and Costal Crdillera. In: Porter TM (ed) Hydrothermal iron oxide copper-gold & related deposits: a global perspective, vol 2. PGC publishing, Adelaine, pp 207–226

Nyström JO, Henríquez F (1994) Magmatic features of iron ores of the Kiruna type in Chile and Sweden: ore textures and magnetite geochemistry. Econ Geol 89:820–839

Oberti R, Ungaretti L, Cannillo E, Hawthorne FC (1993) The mechanism of Cl incorporation in amphibole. Am Mineral 78:746–752

Orville PM (1975) Stability of scapolite in the system Ab-An-NaCl-CaCO$_3$ at 4 kb and 750°C. Geochim Cosmochim Acta 39:1091–1105

Page DC, Watson MD (1976) The Pb-Zn Deposit of Rosh Pinah Mine, South West Africa. Econ Geol 71:306–327

Pearce JA (1996) A User's Guide to Basalt Discrimination Diagrams. In: Wyman DA (ed) Trace element geochemistry of volcanic rocks: applications for massive sulphide exploration. Geological Association of Canada, pp 79–113

Porter TM (eds) (2001) Hydrothermal iron oxide copper-gold & related deposits: a global perspective. Australian Mineral Foundation, Adelaide, p 349

Potts PJ, Bowles JFW, Reed SJB, Cave MR (eds) (1995) Microprobe techniques in the earth sciences. Chapman & Hall, London, pp 419

Quezada R, Ros F (1975) Malmberäkning av Tjårrojåkka järnmalmsfyndighet. Geological Survey of Sweden, BRAP 82569, p 15 (in Swedish)

Raymond LA (1995) Petrology: the study of igneous, sedimentary, and metamorphic rocks. Wm. C. Brown Communications, Inc., Dubuque, p 742

Romer RL, Kjøsnes B, Korneliussen A, Lindahl I, Skyseth T, Stendal M, Sundvoll B (1992) The Archaean-Proterozoic boundary beneath the Caledonides of northern Norway and Sweden: U-Pb, Rb-Sr and ε Nd isotope data from the Rombak-Tysfjord area. Geological Survey of Norway, 91.225, p 67

Romer RL, Martinsson O, Perdahl J-A (1994) Geochronology of the Kiruna iron ores and hydrothermal alterations. Econ Geol 89:1249–1261

Ros F (1979) Tjårrojåkka kopparmalmsfyndighet. Geological Survey of Sweden, BRAP 82 567, p 17 (in Swedish)

Ros F, Rönnbäck L (1971) PM rörande malmobjektet Tjårrojåkka. Geological Survey of Sweden, BRAP 82570, p 2 (in Swedish)

Rosenberg PE, Foit FF Jr (1977) Fe^{2+}-F avoidance in silicates. Geochim Cosmochim Acta 41:345–346

Rubin JN, Henry CD, Price JG (1993) The mobility of zirconium and other "immobile" elements during hydrothermal alteration. Chem Geol 110:29–47

Sandrin A, Elming S-Å (2003) Tectonophysical study of an epigenetic Cu-Fe mineralisation in northern Sweden. GAC-MAC-SEG Joint Annual Meeting. Vancouver, Canada. CD-ROM 0–919216–86–2

Shaw DM (1960) The Geochemistry of Scapolite, Part II. Trace elements, petrology, and general geochemistry. J Petrol 1:261–285

Sillitoe RH (2003) Iron oxide-copper-gold deposits: an Andean view. Miner Deposita 38:787–812

Skiöld T, Öhlander B, Vocke JRD, Hamilton PJ (1988) Chemistry of Proterozoic orogenic processes at a continental margin in northern Sweden. Chem Geol 69:193–207

Spear FS (1993) Metamorphic phase equilibria and pressure-temperature-time paths. Mineralogical Society of America, Washington, p 799

Wanhainen C, Broman C, Martinsson O (2003) The Aitik Cu-Au-Ag deposit in northern Sweden: a product of high salinity fluids. Miner Deposita 38:715–726

Vanko DA, Bishop FC (1982) Occurrence and origin of marialitic scapolite in the Humboldt Lopolith, N.W. Nevada. Contrib Mineral Petrol 81:277–289

Winchester JA, Floyd PA (1977) Geochemical discrimination of different magma series and their differentiation products using immobile elements. Chem Geol 20:325–343

Wing BA, Ferry JM, Harrison TM (2003) Prograde destruction and formation of monazite and allanite during contact and regional metamorphism of pelites: petrology and geochronology. Contrib Mineral Petrol 145:228–250

Witschard F (1984) The geological and tectonic evolution of the precambrian of northern Sweden—a case for basement reactivation? Precamb Res 23:273–315

Zhu C, Sverjensky DA (1991) Partitioning of F-Cl-OH between minerals and hydrothermal fluids. Geochim Cosmochim Acta 55:1837–1858